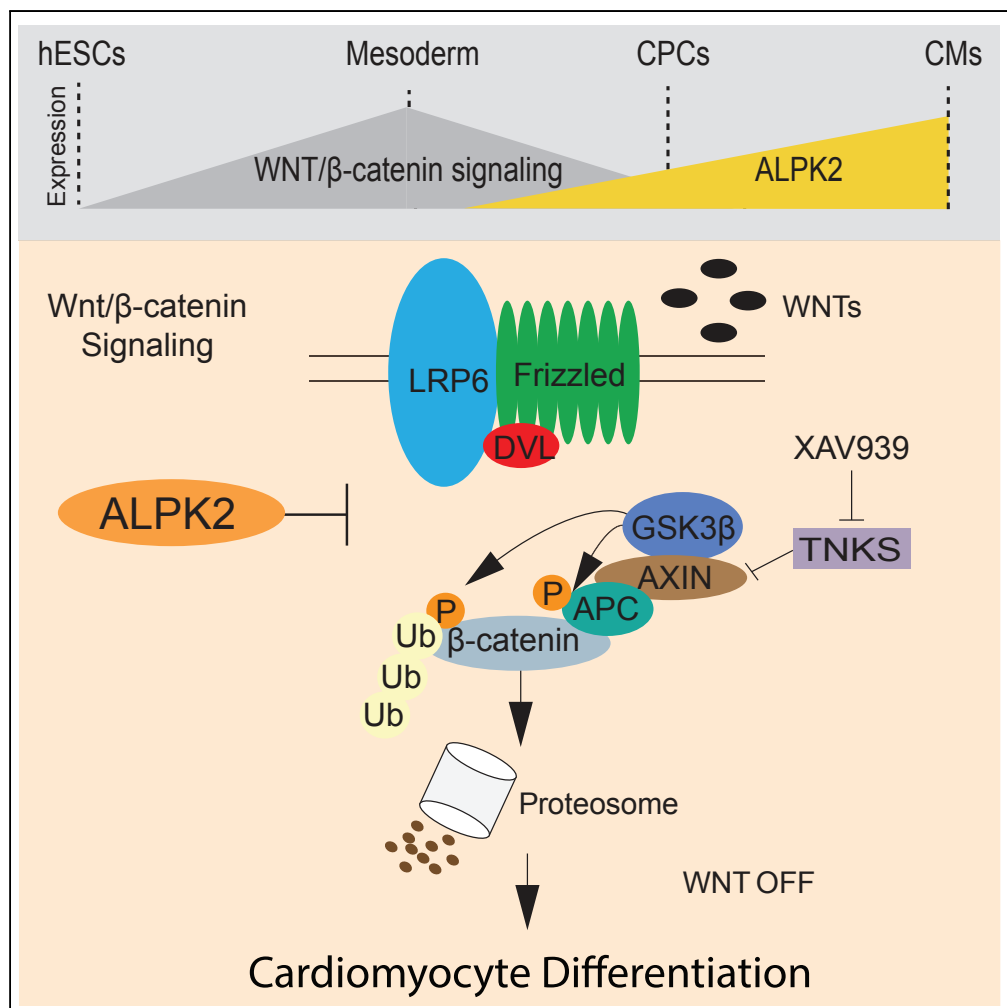**Article**

ALPK2 Promotes Cardiogenesis in Zebrafish and Human Pluripotent Stem Cells

Peter Hofsteen,
Aaron Mark
Robitaille,
Nicholas Strash,
Nathan Palpant,
Randall T. Moon,
Lil Pabon, Charles
E. Murry

peter.hofsteen@promega.
com (P.H.)
murry@uw.edu (C.E.M.)

HIGHLIGHTS
ALPK2 is expressed and
regulated during hESC
cardiomyocyte lineage
determination

Cardiac development in
zebrafish embryos and
hESCs requires ALPK2

ALPK2 negatively
regulates WNT signaling
to promote
cardiomyocyte
differentiation

Article

ALPK2 Promotes Cardiogenesis in Zebrafish and Human Pluripotent Stem Cells

Peter Hofsteen,[1,4,6,*] Aaron Mark Robitaille,[5,6] Nicholas Strash,[1,4,6] Nathan Palpant,[1,4,6,8] Randall T. Moon,[5,6,7] Lil Pabon,[1,4,6] and Charles E. Murry[1,2,3,4,6,9,*]

SUMMARY

Cardiac development requires coordinated biphasic regulation of the WNT/β-catenin signaling pathway. By intersecting gene expression and loss-of-function siRNA screens we identified Alpha Protein Kinase 2 (ALPK2) as a candidate negative regulator of WNT/β-catenin signaling in cardiogenesis. In differentiating human embryonic stem cells (hESCs), ALPK2 is highly induced as hESCs transition from mesoderm to cardiac progenitors. Using antisense knockdown and CRISPR/Cas9 mutagenesis in hESCs and zebrafish, we demonstrate that ALPK2 promotes cardiac function and cardiomyocyte differentiation. Quantitative phosphoproteomics, protein expression profiling, and β-catenin reporter assays demonstrate that loss of ALPK2 led to stabilization of β-catenin and increased WNT signaling. Furthermore, cardiac defects attributed to ALPK2 depletion can be rescued in a dose-dependent manner by direct inhibition of WNT signaling through the small molecule XAV939. Together, these results demonstrate that ALPK2 regulates β-catenin-dependent signaling during developmental commitment of cardiomyocytes.

INTRODUCTION

Directed differentiation from human embryonic stem cells (hESCs) toward cardiomyocytes serves as an *in vitro* model to elucidate regulatory mechanisms during human heart development (Hofsteen et al., 2016; Palpant et al., 2015a). Differentiation of cardiomyocytes requires temporal regulation of the WNT/β-catenin signal transduction pathway (Hofsteen et al., 2016; Lian et al., 2012; Naito et al., 2006; Palpant et al., 2015b; Ueno et al., 2007). Activation of WNT/β-catenin signaling is essential for the exit from pluripotency and mesoderm formation, whereas repression of the pathway is required for the transition toward the cardiomyocyte lineage (Davidson et al., 2012; Hofsteen et al., 2016; Palpant et al., 2015b). Studies have shown that modulation of the Wnt pathway is sufficient to direct cells through stage-specific transition during differentiation (Burridge et al., 2014; Lian et al., 2012). Thus, identifying regulators that inhibit WNT/β-catenin signaling is critical toward understanding human heart development.

WNT/β-catenin signaling is regulated by post-translational modifications of β-catenin (Gao et al., 2014; Moon et al., 2004). A "destruction complex" that contains scaffolding proteins and protein kinases phosphorylates β-catenin to display a motif that is recognized for ubiquitylation and degradation by the proteasome (Stamos and Weis, 2013). Lack of β-catenin phosphorylation activates WNT signaling (Stamos and Weis, 2013). Stabilized β-catenin shuttles into the nucleus and binds to transcription factors, notably TCF/LEF family members, to activate transcription of WNT target genes (Hsu et al., 1998; MacDonald et al., 2009). Continued activation of WNT/β-catenin signaling in the mesoderm represses cardiomyocyte fate and promotes endothelial and hematopoietic fate (Palpant et al., 2015b; wam\Woll et al., 2008). Thus, identifying regulators that inhibit WNT/β-catenin signaling is critical to control cell fate decisions during human heart development.

In the current study, by using combinatorial screening we identified a member of an atypical alpha protein kinase family member, alpha protein kinase 2 (ALPK2), as a cardiac developmental regulator and WNT/β-catenin signaling inhibitor. This protein family shares a highly conserved alpha protein kinase domain and, unlike conventional protein kinases, they are evolutionarily restricted to vertebrates (Middelbeek et al., 2010). There are six alpha kinases: eukaryotic elongation factor 2 kinase (eEF2K), TRP ion channel proteins (TRPM6 and TRPM7) as well as lymphocyte alpha kinase (LAK, or ALPK1), heart alpha kinase (HAK, or ALPK2), and muscle alpha kinase (MAK, or ALPK3), which were named from the tissues they were derived from (Drennan and Ryazanov, 2004; Middelbeek et al., 2010). ALPK2 has known roles in cancer by regulating cell cycle and DNA repair genes (Yoshida et al., 2012) and as a candidate regulator of hypertension

[1]Department of Pathology, School of Medicine, University of Washington, 850 Republican Street, Brotman Building Room 453, Seattle, WA 98109, USA

[2]Department of Bioengineering, School of Medicine, University of Washington, Seattle, WA 98109, USA

[3]Department of Medicine (Division of Cardiology), School of Medicine, University of Washington, Seattle, WA 98109, USA

[4]Center for Cardiovascular Biology, School of Medicine, University of Washington, Seattle, WA 98109, USA

[5]Department of Pharmacology, School of Medicine, University of Washington, Seattle, WA 98109, USA

[6]Institute for Stem Cell and Regenerative Medicine, School of Medicine, University of Washington, Seattle, WA 98109, USA

[7]Howard Hughes Medical Institute, University of Washington, Seattle, WA 98109, USA
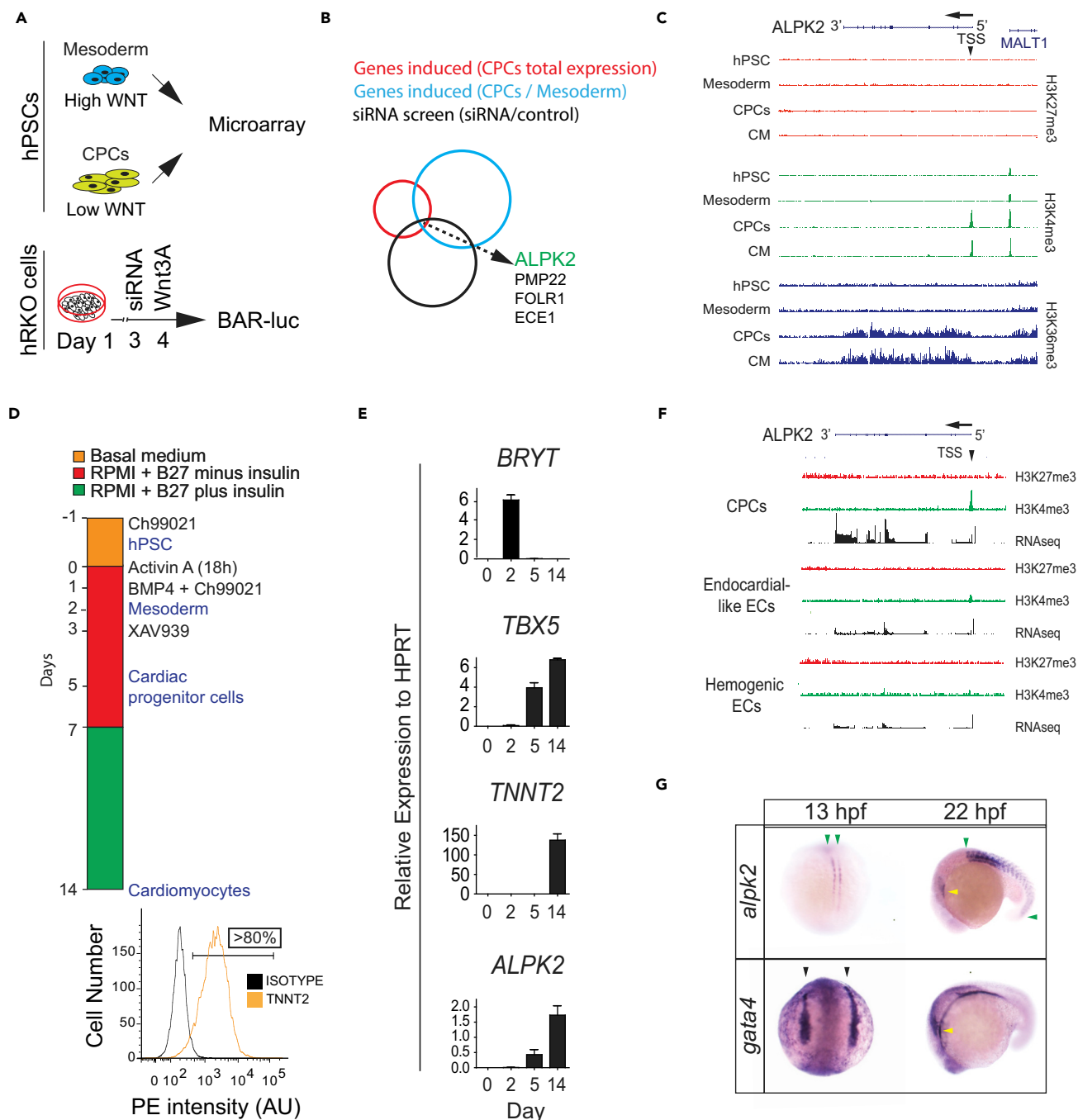
[8]Present address: Australia Centre for Cardiac and Vascular Biology, Institute for Molecular Bioscience, University of Queensland, Brisbane, Australia, QLD, 4067

[9]Lead Contact

*Correspondence: peter.hofsteen@promega.com (P.H.), murry@uw.edu (C.E.M.)

https://doi.org/10.1016/j.isci.2018.03.010

Figure 1. ALPK2 Identification and Expression Analyses

(A) Schematic of combinatorial screening of RNA expression from hESC cardiomyocyte differentiation from human embryonic stem cells (hESCs) coupled with an siRNA screen using β-catenin-activated reporter (BAR)-transduced human RKO colon carcinoma cells (hRKO) stimulated with recombinant Wnt3A.

(B) Venn diagram identifying Alpha Protein Kinase 2 (ALPK2).

(C) Chromatin precipitation followed by deep sequencing (ChIP-Seq) for histone marks H3K4me3, H3K36me3, and H27K4me3 in hESC-derived cultures: hESC (day 0), mesoderm (day 2), cardiac progenitor cells (CPCs, day 5), and cardiomyocytes (day 14) (N = 2).

(D) Protocol for high-density monolayer-directed differentiation of hESC-derived cardiomyocytes yielding a high percentage of cardiac troponin T (TNNT2)-positive cells by flow cytometry.

(E) Quantitative RT-PCR analysis of markers of mesoderm (Brachyury T, *BRYT*), cardiac progenitor cells (T-box 5, *TBX5*), cardiomyocytes (*TNNT2*), and *ALPK2* at days 0, 2, 5, 14 during cardiomyocyte differentiation.

(Chauvet et al., 2011), whereas its role during heart development has not been characterized. Our data indicate that one function of ALPK2 is to negatively regulate WNT/β-catenin signaling during cardiac development in hESCs and zebrafish.

RESULTS

ALPK2 Is Expressed and Regulated during Cardiomyocyte Development

To identify negative regulators of the WNT/β-catenin signaling pathway, we conducted a combinatorial screen comparing previously published RNA expression from hESC-derived mesoderm and cardiac progenitor cells (CPCs) (Paige et al., 2012) with a small interfering RNA (siRNA) screen using human colorectal cancer cells (hRKO) carrying a β-catenin-activated reporter (BAR) driving luciferase (James et al., 2009) (Figure 1A). By intersecting these datasets we identified genes that were highly induced in CPCs that significantly increased BAR activity following siRNA knockdown. This analysis identified a previously unidentified putative cardiac and WNT/β-catenin signaling protein kinase, alpha protein kinase 2 (ALPK2; Figure 1B). ALPK2 was induced 68-fold in CPCs and increased BAR activity by 4-fold following siRNA-mediated knockdown.

We further explored the role of ALPK2 by surveying the epigenetic landscape over a staged time course of cardiomyocyte differentiation from hESCs (Paige et al., 2012). Epigenetic histone modification of chromatin marks H3K4me3 (active promoters) and H3K36me3 (RNA polymerase II activity) show that ALPK2 is epigenetically regulated as cells transition from mesoderm (day 2) to CPCs (day 5) and definitive cardiomyocytes (CMs, day 14) (Figure 1C). Of note, the repressive histone mark, H3K27me3, was not altered throughout the differentiation process (Figure 1C). We aimed to further characterize the expression of ALPK2 and assess its role during heart development. Toward this goal, hESCs were differentiated into cardiomyocytes using a high-density monolayer differentiation protocol (Palpant et al., 2015a). Differentiation of hESCs was induced with Activin A and bone morphogenetic protein 4 (BMP4) coupled with serial small molecule activation and inhibition of canonical WNT/β-catenin signaling (Figure 1D). This directed differentiation protocol typically yields high-purity cardiomyocytes (>80% cardiac troponin T; TNNT2^{+}) as assessed by flow cytometry (Figure 1D). We analyzed transcript abundance in undifferentiated hESCs (day 0), mesodermal cells (day 2), CPCs (day 5), and cardiomyocytes (day 14). Expression of the pan-mesodermal marker Brachyury T (*BRYT*) peaked on day 2 and decreased to baseline levels by day 5. Following the peak of *BRYT* expression, the early cardiac marker T-box 5 (*TBX5*) could be detected at days 5 and 14. Lastly, the sarcomeric gene cardiac troponin T (*TNNT2*) was robustly expressed on day 14. These data indicated that normal mesoderm formation, CPC specification, and cardiomyocyte differentiation occurred. Analysis of *ALPK2* during this time course showed expression starting at day 5 with increasing levels at day 14 (Figure 1E, 2896-fold induction from pluripotency), demonstrating that ALPK2 is temporally expressed during specification of CPCs and cardiac commitment.

We subsequently compared the expression and epigenetic regulation of ALPK2 in three distinct mesodermal progenitor cell lineages (CPCs, endocardial-like endothelial cells [ECs], and hemogenic ECs) to decipher whether ALPK2 was expressed and regulated in non-cardiomyocyte lineages. These populations are generated by specifying distinct mesodermal sub-populations at the onset of differentiation by stimulation with different doses of Activin A and BMP4 as described in the Transparent Methods (Palpant et al., 2015b). We compared RNA sequencing and H3K4me3 and H3K27me3 histone modification at the ALPK2 locus and observed that ALPK2 was highly expressed and regulated in CPCs but not in endocardial-like ECs or hemogenic ECs (Figure 1F) (Palpant et al., 2017). In total, these data indicate ALPK2 is specifically regulated as hESCs differentiate toward the cardiomyocyte lineage.

Zebrafish (*Danio rerio*) are used as an *in vivo* model of heart development owing to the highly conserved developmental mechanisms and genome similarities to humans (Bakkers, 2011; Howe et al., 2013; Stainier and Fishman, 1994). In particular, sequence analyses show that among vertebrates, ALPK2 exhibits a high
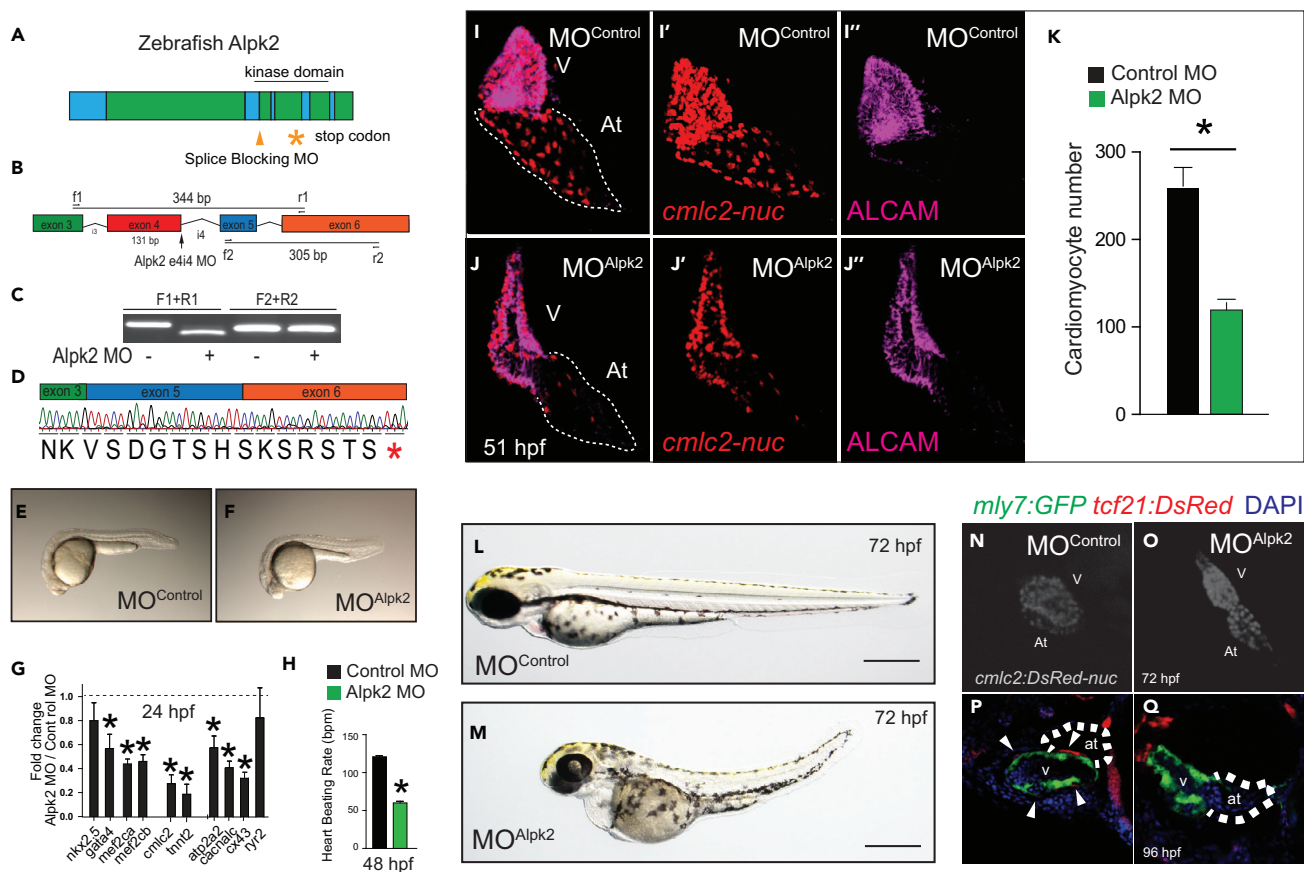
Figure 2. Alpk2 Is Essential for Zebrafish Cardiac Development

(A) Zebrafish Alpk2 locus and targeted region by splice-blocking morpholino oligonucleotides (MO). * denotes stop codon.

(B–D) RT-PCR and Sanger sequencing demonstrating splice-blocking MO caused alternative splicing resulting in a 131-base pair deletion and premature stop codon. * denotes stop codon.

(E and F) Zebrafish injected with negative control MO (E) or Alpk2 MO (F) at 24 hr post fertilization (hpf).

(G and H) Transcript analysis (G) and heart beating rate (H) of control and Alpk2 morphants at 24 and 48 hpf, respectively (N = 5, 15–22 pooled embryos per N).

(I–O) Representative images of control and Alpk2 MO-injected hearts carrying a transgene for *cmlc2:DsRed-nuc* to quantify cardiomyocyte nuclei (K) at 51 hpf (N = 7–9). Red denotes *cmlc2:DsRed-nuc* and magenta is antibody staining for activated leukocyte cell adhesion molecule (ALCAM). Representative bright-field images of control MO (L) and Alpk2 MO (M) injected zebrafish at approximately 72 hpf. Representative images of control MO (N) and Alpk2 MO (O) injected zebrafish hearts carrying a transgene (*cmlc2:DsRed-nuc*) to denote cardiac morphology at approximately 72 hpf.

(P and Q) Confocal images of control and *Alpk2* morphant fish carrying *myl7:GFP* and *tcf21:DsRed* at 96 hpf. White arrowheads denote *tcf21*+ epicardial cells on the heart ventricle. N = 3; independent biological replicates with 45–76 pooled animals per N unless otherwise noted.

Data are mean ± SEM; * denotes p ≤ 0.05.

degree of conservation particularly within the alpha kinase domain (Figure S1). To visualize spatiotemporal expression during whole embryo development we analyzed zebrafish *alpk2* by *in situ* hybridization and compared its expression profile to a cardiac transcription factor, *gata4*. At 13 hr post fertilization (hpf), *gata4* is expressed in the bilateral heart, forming fields of pre-cardiac mesoderm, whereas *alpk2* is expressed in the precursor cells of slow twitch muscle fibers (adaxial cells) of the paraxial mesoderm. At 22 hpf, *gata4* and *alpk2* are co-expressed in the developing heart (Figure 1G). Thus ALPK2 is expressed during cardiac development *in vivo* and *in vitro*.

Depletion of Alpk2 Impairs Zebrafish Heart Development

We next sought to determine the role of ALPK2 *in vivo* by depleting Alpk2 in zebrafish using splice-blocking morpholino oligonucleotides (MO). Injection of Alpk2 MOs caused alternative splicing and exon 4 removal to create a premature stop codon in exon 6 (Figures 2A–2D). Alpk2 morphants showed no observable structural defects at 24 hpf when compared with animals injected with scrambled negative control MOs (Figures
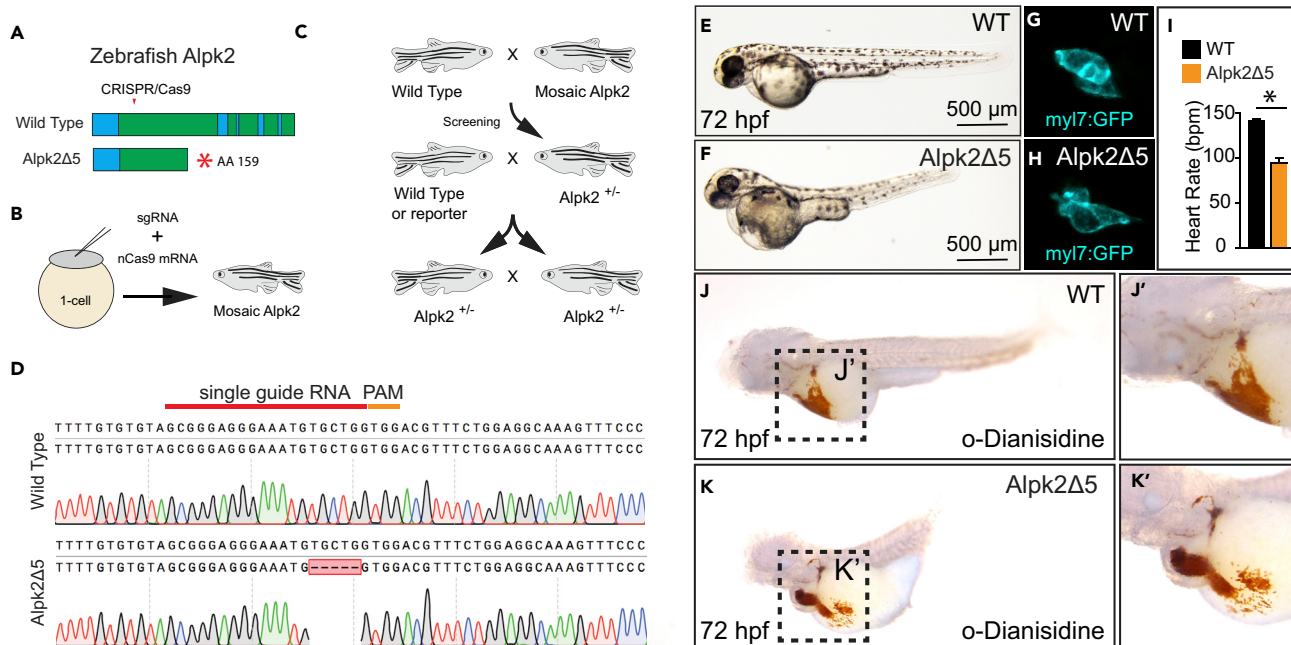
Figure 3. CRISPR/Cas9 Knockout of Zebrafish Alpk2 Inhibits Cardiac Development

(A) Schematic of the zebrafish Alpk2 locus and CRISPR/Cas9 targeted region. * denote stop codon.

(B and C) Injection and breeding paradigm to generate Alpk2 null homozygosity.

(D–H) (D) Sanger sequencing of homozygous mutation showing 5-bp deletion. Representative bright-field (E, F; 72 hpf) and fluorescent (G, H; 120 hpf) images of wild-type (E, G) and Alpk2 null zebrafish (F, H) carrying a transgene for *myl7:GFP* (G, H).

(I) Quantification of cardiac beating rate comparing Alpk2 null zebrafish to wild-type siblings at 72 hpf. * denotes p ≤ 0.05.

(J and K) Representative bright-field images of hemoglobin-peroxidase staining with *o*-Dianisidine in 72 hpf WT and homozygous Alpk2Δ5 embryos. Data are representative of N ≥ 3 independent breeding experiments consisting of n∼30–150 embryos per spawn. hpf, hours post fertilization.

2E and 2F). However, transcriptional profiling of a panel of genes with known roles in early heart development (*nkx2.5, gata4, mef2ca, mef2cb, cmlc2, tnnt2, atp2a2, cacnalc2, cx43,* and *ryr2*) revealed that Alpk2 morphants had significantly reduced mRNA expression in all transcripts except *nkx2.5* and *ryr2* at 24 hpf (Figure 2G). At 48 hpf, Alpk2 morphants showed a significantly reduced heart beating rate (control 120.0 ± 1.29 bpm; alpk2 MO2 60.0 ± 2.19 bpm; Figure 2H) and cardiomyocyte numbers (*cmlc2:DsRed-nuc;* control 259 ± 21, *Alpk2 MO* 119 ± 8; 51 hpf; Figures 2I–2K). Of note, no difference in staining of endothelial cells was observed on the basis of activated leukocyte cell adhesion molecule (ALCAM; Figures 2I–2K). By 72 hpf, Alpk2 morphants displayed pericardial and yolk sac effusion and pronounced cardiac malformation coupled with defects in posterior development (Figures 2L–2O). We also assessed epicardium formation in fish lacking Alpk2 using zebrafish carrying a florescence epicardial cell reporter (*tcf21:DsRed* (Kikuchi et al., 2011). The zebrafish epicardium is the serosal epithelial lining of the heart derived from an extra-cardiac source of cells termed the proepicardium that is located adjacent to the pericardial sac and the venus pole during primitive heart tube formation (Plavicki et al., 2014; Serluca, 2008) and requires normal cardiac fitness to form (Peralta et al., 2013; Plavicki et al., 2014). In contrast to controls, Alpk2 morphants lacked *tcf21*[+] ventricular epicardium at 96 hpf. During normal development, this is a time when the epicardium envelops the zebrafish heart ventricle but not the atrium (Figures 2P and 2Q; white arrowheads) (Plavicki et al., 2014).

There remains controversy regarding the use of MOs to study gene function (Rossi et al., 2015; Schulte-Merker and Stainier, 2014). To address this, we used CRISPR/Cas9 mutagenesis to induce indel mutations in exon 2 of Alpk2. Pilot studies indicated that the F0 fish had significant cardiac defects and posterior developmental anomalies that phenocopied the MO experiments. To avoid possible artifacts associated with mosaic mutations in the injected embryos, we derived an F1 line of fish with a heterozygous 5-base pair frameshift mutation within exon 2 of Alpk2 that resulted in a premature stop codon at amino acid 159 (Alpk2Δ5, Figures 3A–3D). Heterozygous fish showed no obvious developmental phenotype and were crossed to generate F2 homozygous Alpk2Δ5 fish. As with the Alpk2 morphants, there was no overt

phenotype observed at 24 hpf in homozygous Alpk2Δ5 mutants. However, following heart tube formation, Alpk2Δ5 homozygotes display pericardial and yolk sac effusion, pronounced cardiac malformation coupled with reduced heart beating rate (Figures 3E–3I). Of note, cardiomyocyte numbers were not assessed in Alpk2Δ5 fish. Hemoglobin-peroxidase staining with *o*-Dianisidine shows that Alpk2Δ5 fish form erythrocytes but they lack blood circulation in the caudal trunk (Figures 3J–3K'). This suggests circulation defects that are secondary to reduced heart function. These results indicate that Alpk2 plays an important role in determining the number of cardiomyocytes, normal cardiac morphology, epicardium formation, and cardiac function.

ALPK2 Promotes Differentiation of hESC-derived Cardiomyocytes

To determine whether ALPK2 plays a functional role in human cardiomyocyte development, ALPK2 was knocked down (KD) by lentiviral short hairpin RNAs (shRNA) in hESCs (Figures 4A and 4B), and cells were subjected to cardiomyocyte differentiation. ALPK2 KD significantly diminished ALPK2 expression throughout the differentiation process (Figure 4C) without disrupting hESC colony morphology or pluripotency-associated gene expression (Figure 4D). To assess the role of ALPK2 during early developmental stages, transcript abundance of markers of mesoderm, CPCs, and definitive cardiomyocytes were assessed on days 2, 5, and 14 of differentiation (Figure 1D). Although there was no change in the expression of the pan-mesoderm marker, *BRYT*, expression of CPC markers, *TBX5* and Islet 1 (*ISL1*), and *TNNT2* was downregulated in ALPK2 KD cells (Figures 4E–4H). In addition, ALPK2 KD cells preferentially differentiated toward a *TNNT2*-negative and smooth muscle actin (SMA)-positive cell type (Figures 4I–4L). These data suggest ALPK2 plays a role during transitioning from mesoderm toward the cardiomyocyte lineage. To further test this hypothesis, we assessed the differentiation efficiency of ALPK2 KD in forming endocardial-like EC and hemogenic EC from mesodermal sub-populations. These results showed no effect on the percentage of endocardial-like or hemogenic ECs (based on KDR/CD34 expression on day 5 of differentiation, Figure S2), indicating ALPK2 specifically plays a role in potentiating the cardiomyocyte lineage.

We characterized potential downstream effectors of ALPK2 by performing label-free quantitative (LFQ) proteomics in hESCs undergoing cardiac-directed differentiation (Figure S3A, Table S2: All proteins identified by LFQ proteomics. Related to Figure 4). To assess the effect on early cardiac cell fate specification, hESCs were transduced with either control or ALPK2 shRNAs and analyzed as hESCs or after differentiation as CPCs. Normalized protein digests were measured by nano-liquid chromatography-tandem mass spectrometry (LC-MS/MS) on a Fusion Orbitrap mass spectrometer and quantified using label-free methods (Hofsteen et al., 2016). Label-free quantification was reproducible across all samples, with an average Pearson's correlation of 0.90 (Figure S3B; representative image). To validate our approach, we analyzed TNNT2 and ALPK2 protein expression over hESC cardiomyocyte differentiation. As expected, both TNNT2 and ALPK2 protein levels increased as cells differentiated toward cardiomyocytes (Figures S3C and S3D). ALPK2 protein expression increased progressively as control hESCs differentiated into CPCs and then into cardiomyocytes, paralleling the mRNA expression pattern. Following treatment with ALPK2 shRNA lentiviruses, ALPK2 protein was decreased in CPCs and cardiomyocytes (Figure S3D).

Next, we performed unbiased hierarchal cluster analysis of samples and found replicates and experimental conditions cluster together (Figure S3E). We analyzed ALPK2-regulated proteins by using p ≤ 0.05 and a cutoff of 2-fold (log2) change. This analysis identified 241 ALPK2-regulated proteins in CPCs (126 upregulated, 115 downregulated; Figure 4M, Table S3: ALPK2-regulated proteins identified by LFQ proteomics in cardiac progenitor cells. Related to Figure 4). We observed no ALPK2-regulated proteins between control and ALPK2 KD undifferentiated hESCs. Gene ontology (GO) term analysis revealed that ALPK2 regulates processes involved in RNA and protein binding, protein kinase binding, cell-cell adhesion, the extracellular matrix, and actin filaments and function, and canonical WNT signaling (Tables S4: GO Terms enriched by ALPK2 knockdown identified by LFQ proteomics in cardiac progenitor cells. Related to Figure 4, Table S5: GO Terms repressed by ALPK2 knockdown identified by LFQ proteomics in cardiac progenitor cells. Related to Figure 4). Specifically, ALPK2 KD reduced TNNT2 and GATA4 expression in CPCs (Figure 4N) and induced the expression of the WNT/β-catenin antagonist and secreted frizzled-related protein (sFRP1) (Ren et al., 2013) as well as the WNT signaling transducer β-catenin (CTNNB1) (Figure 4N). These proteomic data suggest ALPK2 regulates key mediators of the WNT/β-catenin signaling pathway and cardiac developmental proteins during cardiomyocyte differentiation.
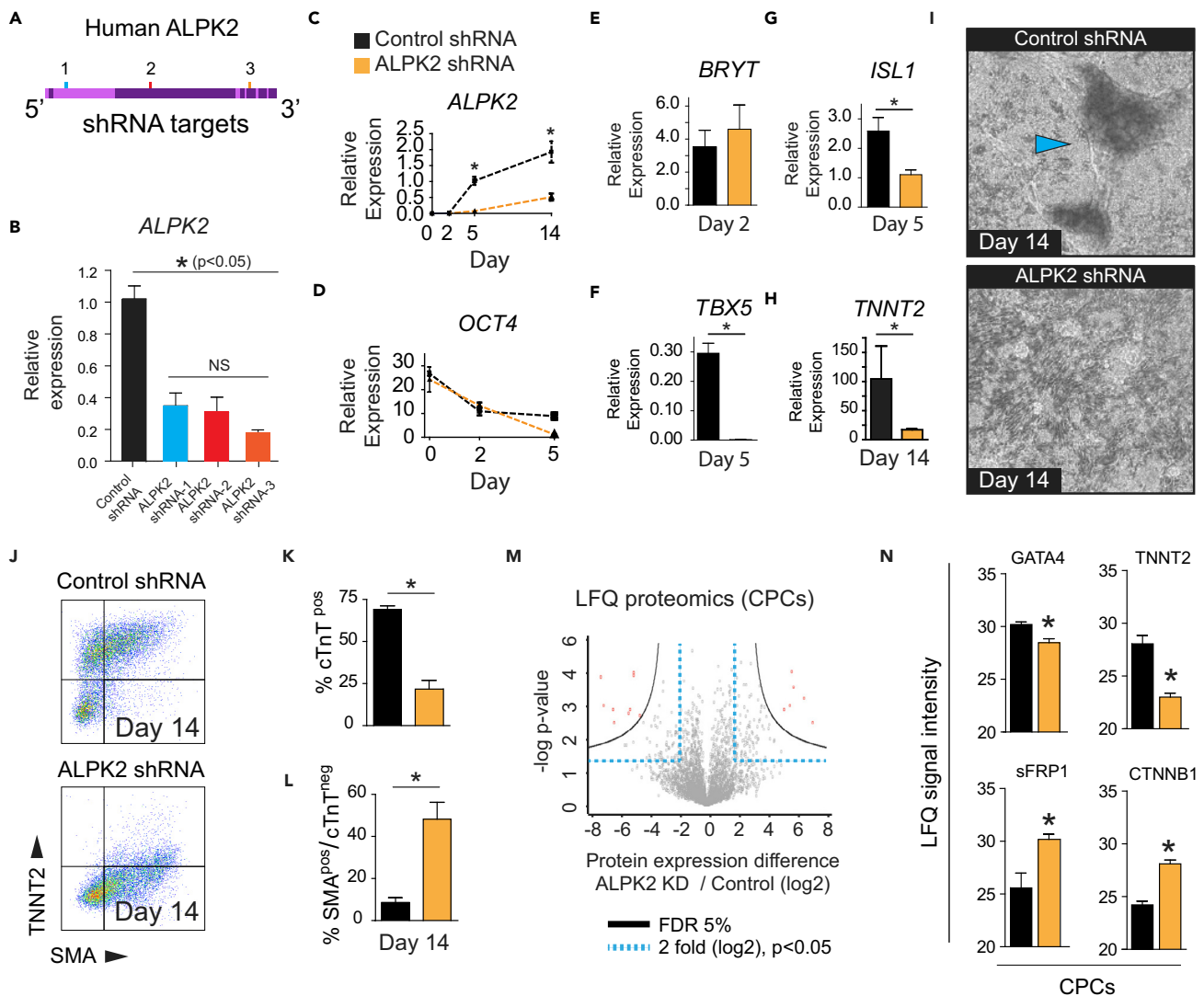
Figure 4. ALPK2 shRNA Knockdown Inhibits Cardiomyocyte Differentiation from hESCs

(A) Schematic of ALPK2 locus and shRNA target sites.

(B–D) (B) Validation of three ALPK2 shRNAs in human embryonic stem cell (hESC)-derived cardiomyocytes by qRT-PCR 3 days following viral transfection. Transcript expression analysis of *ALPK2* (C) and *OCT4* (D) following control or ALPK2 lentiviral shRNA transfection over a time course of cardiomyocyte differentiation.

(E–H) RT-qPCR analysis of mesoderm (*BRYT*), primary (*TBX5*) and secondary (*ISL1*) heart field genes, and the cardiac structural gene (*TNNT2*).

(I) Representative bright-field images of control and ALPK2 shRNA-treated cells following directed differentiation toward cardiomyocytes (day 14). Arrowhead denotes contractile cardiomyoctes.

(J–L) Flow cytometry (y axis, TNNT2; x axis, smooth muscle actin, SMA) on differentiation day 14 following control and ALPK2 shRNA lentiviral transduction (N = 3).

(M) Volcano plot of comparing cardiac progenitor cells (CPCs) transfected with control or ALPK2 shRNAs by system-wide label-free quantitative proteomics (FDR, false discovery rate).

(N) Protein expression of TNNT2, GATA4, sFRP1, and CTNNB1 (LFQ signal intensity; log2 transformed) in control and ALPK2 shRNA CPCs derived from hESCs. Proteomic data are representative of two biological replicates that were pooled, processed, and measured in triplicate.

Data are mean ± SEM; * denotes p ≤ 0.05; LFQ, label-free quantification. See also Figures S2 and S3.

ALPK2 Negatively Regulates WNT/β-Catenin for Cardiac Development

The LFQ proteomics indicate that ALPK2 knockdown affects WNT/β-catenin signaling during cardiac development. To more definitively assess the role of ALPK2 in regulating WNT/β-catenin signaling, we stably transduced a lentiviral BAR driving venus expression in hESCs (Figure S4A). BAR-hESCs were subsequently transduced with control or ALPK2 shRNAs and were subjected to directed differentiation toward
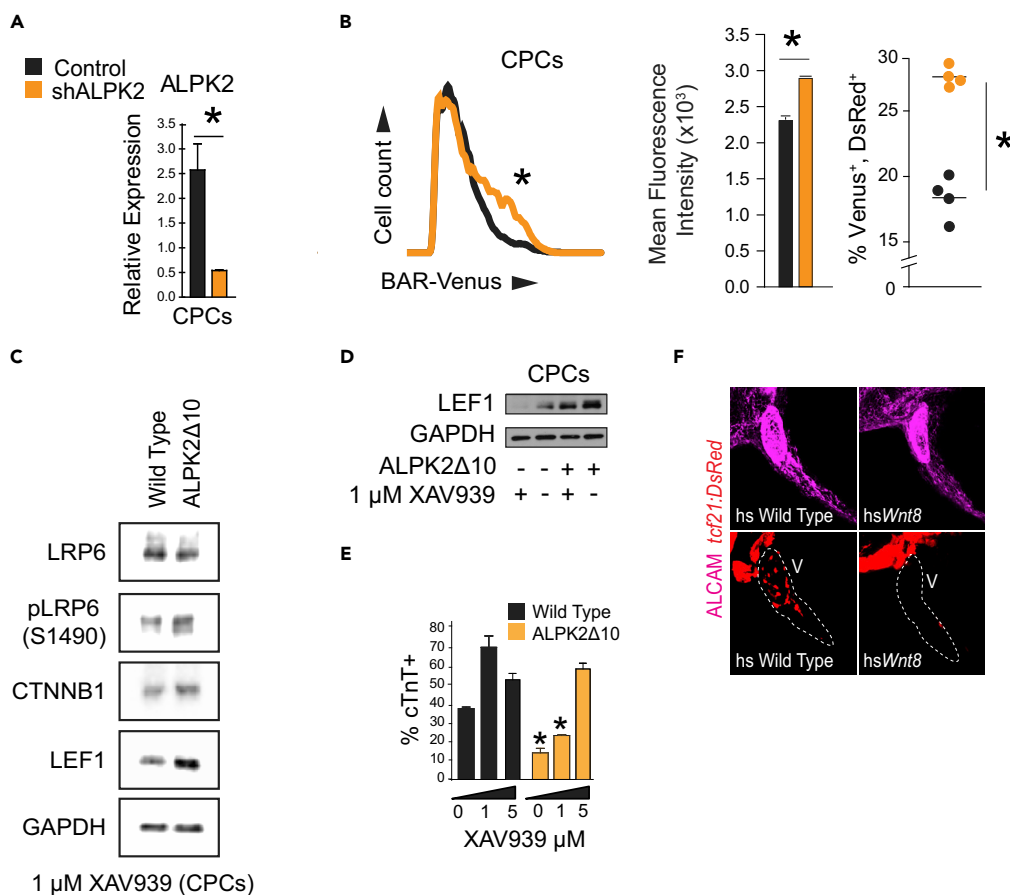
Figure 5. ALPK2 Inhibits WNT/β-Catenin Signaling to Promote Cardiogenesis

(A) Transcripts abundance of *ALPK2* in control and ALPK2 shRNA-transfected cardiac progenitor cells (CPCs) derived from human embryonic stem cells (hESCs).

(B) Flow cytometric plot and graphs quantifying venus expression driven by β-catenin activated reporter (BAR) in live CPCs following control or ALPK2 shRNA transfection as hESCs.

(C) Western blot protein expression analysis of WNT/β-catenin signaling modulators in wild-type and CRISPR/Cas9-mediated ALPK2 mutant hESC-derived CPCs (ALPK2Δ10) treated with a small molecule direct tankyrase inhibitor XAV939 (1 μM).

(D) Western blotting for the WNT/β-catenin signaling target LEF1 in wild-type and ALPK2Δ10 cells with or without the addition of XAV939 (0 or 1 μM).

(E) TNNT2 flow cytometry quantification of day 14 cardiomyocytes derived from wild-type and ALPK2Δ10 hESCs treated with XAV939 (0, 1, 5 μM).

(F) Representative images of heat shocked (hs) wild-type and hsWnt8b transgenic zebrafish carrying a transgene for the epicardium (*tcf21:DsRed*) at 96 hpf. Fish were counterstained with an activated leukocyte cell adhesion molecule (ALCAM; magenta).

N = 3–5 biological replicates, and data are displayed as mean $\pm$ SEM. * = p $\leq$ 0.05. See also Figure S4.

CPCs, followed by assessment of venus expression analysis by live-cell flow cytometry (Figure S4B). ALPK2 KD significantly reduced *ALPK2* expression (Figure 5A) and increased the overall mean live-cell venus fluorescence intensity (geometric mean: control, $2.39 \pm 0.03 \times 10^3$; ALPK2 KD, $3.01 \pm 0.44 \times 10^3$) and significantly increased the percentage of venus-expressing CPCs (venus$^+$/DsRed$^+$; control %, 18.4 ± 0.8; ALPK2 KD %, 27.6 ± 0.4) (Figure 5B), indicating ALPK2 KD increases β-catenin-dependent WNT signaling.

To further assess the role of ALPK2 and WNT/β-catenin signaling we used CRISPR/Cas9 gene editing to mutate the protein kinase domain of ALPK2 in hESCs. This approach successfully created an hESC line carrying a homozygous 10-bp frameshift deletion causing a premature stop codon in exon 9 (ALPK2Δ10; Figures S4C and S4D). Wild-type and ALPK2Δ10 hESCs were differentiated to CPCs (Figure 1D), and transcript

abundance of *ALPK2* was measured by RT-qPCR. ALPK2Δ10 CPCs had a significantly reduced *ALPK2* expression when compared with control (Figure S4E), suggesting ALPK2Δ10 cells undergo nonsense-mediated mRNA decay. ALPK2Δ10 and wild-type hESCs were subsequently differentiated toward cardio-myocytes as described in Figure 1D and analyzed by immunoblotting and TNNT2 flow cytometry on days 5 and 14, respectively. We characterized the expression of LRP6, pLRP6, CTNNB1, and LEF1 as indicators of active WNT/β-catenin signaling in CPCs lacking ALPK2. The WNT co-receptor, LRP6, is phosphorylated by glycogen synthase kinase 3 beta (GSK3β) and casein kinase 1 (CK1) upon WNT ligand binding (Davidson et al., 2005; Zeng et al., 2005). Furthermore, induction of WNT/β-catenin signaling is associated with induced expression of target proteins such as LEF1 (Hsu et al., 1998). The expression of pLRP6, CTNNB1, and LEF1 proteins was increased in ALPK2Δ10 CPCs when compared with wild-type CPCs (Figure 5C). To further examine the role of ALPK2 during WNT/β-catenin signaling we analyzed the expression of LEF1 using wild-type and ALPK2Δ10 CPCs with or without a small molecule WNT/β-catenin signaling inhibitor, XAV939 (0 or 1 μM). In wild-type cells, XAV939 reduced LEF1 expression to almost undetectable levels. Although baseline LEF1 levels are increased in ALPK2Δ10 CPCs, treatment with XAV939 also reduced LEF1 protein abundance (Figure 5D), suggesting that at least part of the ALPK2's Wnt-suppression effect occurs upstream of the Axin-stabilizing enzyme, tankyrase, the target for XAV939 (Huang et al., 2009).

Next, we sought to rescue the ALPK2-mediated cardiomyocyte differentiation defects by attenuating WNT/β-catenin signaling with increasing doses of the pathway inhibitor, XAV939. Wild-type and ALPK2Δ10 cells were exposed to 0, 1, and 5 μM XAV939 on day 3 of the differentiation protocol for 2 days, and cells were collected on day 14 for flow cytometry analysis (TNNT2). XAV939 showed a dose-dependent ability to restore the cardiogenic potential of ALPK2Δ10 cells, such that exposure to 5 μM XAV939 restored cardiac differentiation to wild-type levels (Figure 5E). Thus inhibition of WNT/β-catenin signaling can restore cardiomyocyte differentiation deficiencies observed in ALPK2Δ10 cells.

WNT/β-catenin signaling pathway modulation is required for the differentiation of the epicardium in hESCs (Bao et al., 2016; Iyer et al., 2015), and Alpk2-depleted zebrafish showed impaired formation of the epicardium (Figure 2). To test more specifically for a role of WNT/β-catenin signaling in epicardium formation in zebrafish, we genetically overexpressed *wnt8* to induce canonical WNT signaling using a heat-shock-inducible zebrafish line (*hsp70:wnt8b-GFP* [Weidinger et al., 2005]) crossed to an epicardial cell reporter (*tcf21:DsRed*). Fish were subjected to heat shock following heart tube formation (24 and 48 hpf), and epicardial formation was assessed at 96 hpf. As with zebrafish depleted of Alpk2, late embryo-larval activation of WNT/β-catenin signaling inhibited the formation of the epicardium (Figure 5F). Collectively, these data demonstrate that inhibition of WNT/β-catenin signaling by ALPK2 is required for the formation of both the myocardium and epicardium.

Quantitative Phosphoproteomics Reveals Phosphorylation Motif and Candidate Substrate Proteins for ALPK2

To identify ALPK2 targets we conducted quantitative phosphoproteomics comparing wild-type with ALPK2Δ10 CPCs (see Transparent Methods in Supplemental Information and Figure 6A). Wild-type and ALPK2Δ10 CPCs were collected and processed for proteomics and phosphoproteomics following stable isotope labeling with amino acids in cell culture (SILAC) and directed differentiation. We detected 2,664 proteins, of which 317 (157 induced, 160 repressed) were differentially expressed (≥2-fold; log2; Figures 6B and S5, and Table S6: All proteins identified by SILAC proteomics. Related to Figure 6). GO term analysis revealed that ALPK2-regulated proteins have known roles in negative regulation of WNT/β-catenin signaling and β-catenin-TCF complex assembly along with proteins that play roles in regulating heart development and actin behavior and function (Figure 6C, Table S7: GO Terms enriched in ALPK2Δ10 cardiac progenitor cells identified by SILAC proteomics. Related to Figures 6 and S8: GO Terms repressed in ALPK2Δ10 cardiac progenitor cells identified by SILAC proteomics. Related to Figure 6).

We validated the proteomics screen by immunoblotting for two proteins with known roles in modulating canonical and non-canonical WNT signaling. Protein kinase N2 (PKN2) has previously been described as a negative regulator of WNT/β-catenin signaling (James et al., 2013) and was predicted to be upregulated in CPCs derived from ALPK2Δ10 hESCs. Alternatively, the cell polarity and non-canonical WNT signaling regulator, Scribble (SCRIB) (Sisson et al., 2015), was predicted to be unchanged in ALPK2Δ10 CPCs. Western blotting for PKN2 and SCRIB confirmed that in ALPK2Δ10 CPCs, PKN2 was upregulated and SCRIB was not changed (Figure 6B).
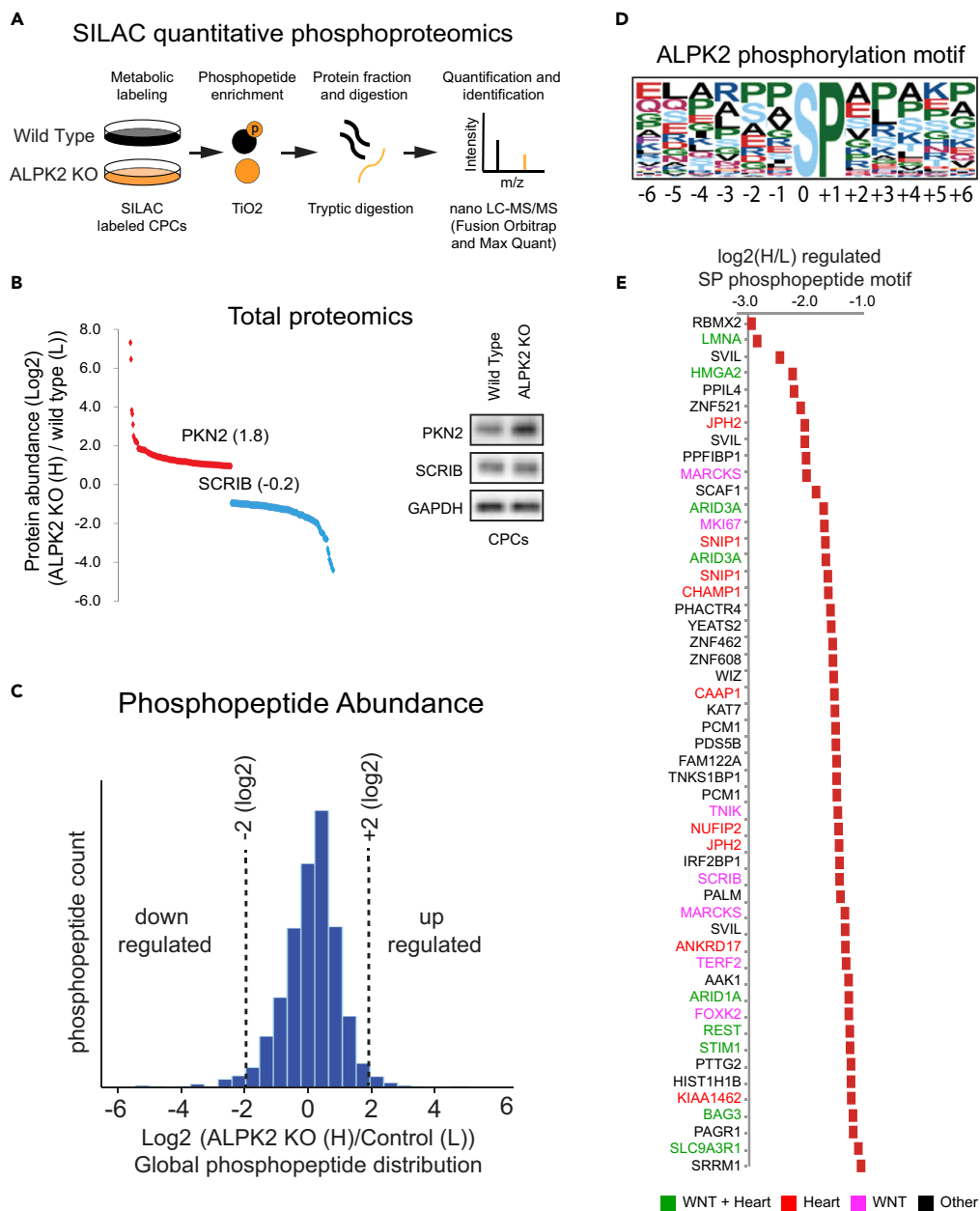
Figure 6. Quantitative Phosphoproteomics Reveals Phosphorylation Motif and Candidate Substrate Proteins for ALPK2

(A) Schematic of stable isotope labeling of amino acids in cell culture (SILAC) quantitative phosphoproteomics using wild-type and ALPK2Δ10 cardiac progenitors differentiated from human embryonic stem cells (hESCs).

(B, left) Waterfall plot of differential protein abundance comparing wild-type and ALPK2Δ10 CPCs. (B, right) Western blot for Protein Kinase N2 (PKN2) and Scribble (SCRIB), N = 3 independent differentiations.

(C) Total distribution of phosphopeptide abundance comparing wild-type and ALPK2Δ10 CPCs.

(D and E) Putative ALPK2 phosphorylation substrate motif and (E) proteins lacking phosphorylation events as a result of ALPK2 mutation. Proteins are color coded indicating their role(s) in both WNT signaling and heart development or disease (green), heart development or disease (red), WNT only (magenta), or other (black). See also Figure S5.

We also detected and quantified 1,972 phosphopeptides corresponding to 846 proteins (Figure 6C, Table S9: All phosphopeptides identified and differentially phosphorylated in ALPK2Δ10 cardiac progenitor cells identified by SILAC proteomics. Related to Figure 6). Phosphorylation motif analysis revealed that

ALPK2 is predicted to target proteins carrying serine-proline amino acid residues (Figure 6D). Of the predicted ALPK2 target substrates (proteins that lack phosphorylation in ALPK2Δ10 CPCs), approximately one-third have known roles in regulating WNT/β-catenin signaling (32.6%) and heart development and disease (34.7%, Figure 6E). Thus our data support the hypothesis that ALPK2 regulates cardiac development by phosphorylating substrates that are associated with WNT/β-catenin signaling during heart development.

DISCUSSION

Regulation of WNT/β-catenin signaling has long been known to be essential for heart development, homeostasis, and disease (Hofsteen et al., 2016; Moon et al., 2004, 2017; Ozhan and Weidinger, 2015; Ueno et al., 2007). We used targeted combinatorial screening from cardiomyocyte differentiation of hESCs coupled with siRNA screen of human cancer cells to identify previously unknown regulators of heart development and WNT/β-catenin signaling. In this study, we demonstrate that knockdown and knockout of ALPK2 in vivo and in vitro result in diminished cardiogenesis and increased WNT/β-catenin signaling activity. ALPK2 is highly expressed in a stage-dependent manner during cardiogenesis and is an important regulator of cardiomyocyte differentiation in hESCs and cardiac development in zebrafish. Furthermore, we find that ALPK2 regulates cardiogenesis by repressing WNT/β-catenin signaling following cardiac commitment. We sought to understand how ALPK2 regulates WNT/β-catenin signaling during cardiogenesis by performing quantitative proteomic screens. These screens further supported our combinatorial efforts by identifying that ALPK2 regulates cardiac proteins along with mediators of the WNT/β-catenin signaling pathway. We consistently observe an increased expression of proteins that inhibit WNT/β-catenin signaling following depletion of ALPK2. Key examples of this are the canonical WNT proteins, PKN2, and sFRP1 that could very likely be induced as a compensatory mechanism to repress the pathway.

Comparing multiple model systems to understand gene function is critical owing to gene duplication, species variation, or compensatory mechanisms (Jensen et al., 2013; Olson, 2006; Rossi et al., 2015). Expression analyses of alpk2 in zebrafish embryos demonstrate that it is expressed in the developing heart, whereas in human ESCs, ALPK2 is expressed in the cardiac progenitor cells and cardiomyocytes. Correspondingly, both model systems show significant defects in cardiogenesis when ALPK2 is knocked down or knocked out.

Taken together, the vertebrate heart requires precise control of signaling cascades to orchestrate dynamic cell fate decisions and morphogenetic changes during development. We identified that the regulation of the WNT/β-catenin signaling pathway by ALPK2 plays a critical role in hESC-CM differentiation and in cardiac maturation in zebrafish. Thus we report ALPK2 is an evolutionarily conserved alpha protein kinase that is important for the earliest stages of vertebrate heart development through repression of WNT/β-catenin signaling.

METHODS

All methods can be found in the accompanying Transparent Methods supplemental file.

SUPPLEMENTAL INFORMATION

Supplemental Information includes Transparent Methods, five figures, and nine tables and can be found with this article online at https://doi.org/10.1016/j.isci.2018.03.010.

ACKNOWLEDGMENTS

iScience

CellPress

AUTHOR CONTRIBUTIONS

DECLARATION OF INTERESTS

REFERENCES

Bakkers, J. (2011). Zebrafish as a model to study cardiac development and human cardiac disease. Cardiovasc. Res. 91, 279–288.

Bao, X., Lian, X., Hacker, T.A., Schmuck, E.G., Qian, T., Bhute, V.J., Han, T., Shi, M., Drowley, L., Plowright, A., et al. (2016). Long-term self-renewing human epicardial cells generated from pluripotent stem cells under defined xeno-free conditions. Nat. Biomed. Eng. 1, https://doi.org/10.1038/s41551-016-0003.

Burridge, P.W., Matsa, E., Shukla, P., Lin, Z.C., Churko, J.M., Ebert, A.D., Lan, F., Diecke, S., Huber, B., Mordwinkin, N.M., et al. (2014). Chemically defined generation of human cardiomyocytes. Nat. Methods 11, 855–860.

Chauvet, C., Crespo, K., Ménard, A., Wu, Y., Xiao, C., Blain, M., Roy, J., and Deng, A.Y. (2011). α-Kinase 2 is a novel candidate gene for inherited hypertension in Dahl rats. J. Hypertens. 29, 1320–1326.

Davidson, G., Wu, W., Shen, J., Bilic, J., Fenger, U., Stannek, P., Glinka, A., and Niehrs, C. (2005). Casein kinase 1 gamma couples Wnt receptor activation to cytoplasmic signal transduction. Nature 438, 867–872.

Davidson, K.C., Adams, A.M., Goodson, J.M., McDonald, C.E., Potter, J.C., Berndt, J.D., Biechele, T.L., Taylor, R.J., and Moon, R.T. (2012). Wnt/β-catenin signaling promotes differentiation, not self-renewal, of human embryonic stem cells and is repressed by Oct4. Proc. Natl. Acad. Sci. USA 109, 4485–4490.

Drennan, D., and Ryazanov, A.G. (2004). Alpha-kinases: analysis of the family and comparison with conventional protein kinases. Prog. Biophys. Mol. Biol. 85, 1–32.

Gao, C., Xiao, G., and Hu, J. (2014). Regulation of Wnt/β-catenin signaling by posttranslational modifications. Cell Biosci. 4, 13.

Hofsteen, P., Robitaille, A.M., Chapman, D.P., Moon, R.T., and Murry, C.E. (2016). Quantitative proteomics identify DAB2 as a cardiac developmental regulator that inhibits WNT/β-catenin signaling. Proc. Natl. Acad. Sci. USA 113, 1002–1007.

Howe, K., Clark, M.D., Torroja, C.F., Torrance, J., Berthelot, C., Muffato, M., Collins, J.E., Humphray, S., McLaren, K., Matthews, L., et al. (2013). The zebrafish reference genome sequence and its relationship to the human genome. Nature 496, 498–503.

Hsu, S.C., Galceran, J., and Grosschedl, R. (1998). Modulation of transcriptional regulation by LEF-1 in response to Wnt-1 signaling and association with beta-catenin. Mol. Cell. Biol. 18, 4807–4818.

Huang, S.M., Mishina, Y.M., Liu, S., Cheung, A., Stegmeier, F., Michaud, G.A., Charlat, O., Wiellette, E., Zhang, Y., Wiessner, S., et al. (2009). Tankyrase inhibition stabilizes axin and antagonizes Wnt signalling. Nature 461, 614–620.

Iyer, D., Gambardella, L., Bernard, W.G., Serrano, F., Mascetti, V.L., Pedersen, R.A., Talasila, A., and Sinha, S. (2015). Robust derivation of epicardium and its differentiated smooth muscle cell progeny from human pluripotent stem cells. Development 142, 1528–1541.

James, R.G., Biechele, T.L., Conrad, W.H., Camp, N.D., Fass, D.M., Major, M.B., Sommer, K., Yi, X., Roberts, B.S., Cleary, M.A., et al. (2009). Bruton's tyrosine kinase revealed as a negative regulator of Wnt-beta-catenin signaling. Sci. Signal. 2, ra25.

James, R.G., Bosch, K.A., Kulikauskas, R.M., Yang, P.T., Robin, N.C., Toroni, R.A., Biechele, T.L., Berndt, J.D., von Haller, P.D., Eng, J.K., et al. (2013). Protein kinase PKN1 represses Wnt/β-catenin signaling in human melanoma cells. J. Biol. Chem. 288, 34658–34670.

Jensen, B., Wang, T., Christoffels, V.M., and Moorman, A.F. (2013). Evolution and development of the building plan of the vertebrate heart. Biochim. Biophys. Acta 1833, 783–794.

Kikuchi, K., Gupta, V., Wang, J., Holdway, J.E., Wills, A.A., Fang, Y., and Poss, K.D. (2011). tcf21+ epicardial cells adopt non-myocardial fates during zebrafish heart development and regeneration. Development 138, 2895–2902.

Lian, X., Hsiao, C., Wilson, G., Zhu, K., Hazeltine, L.B., Azarin, S.M., Raval, K.K., Zhang, J., Kamp, T.J., and Palecek, S.P. (2012). Robust cardiomyocyte differentiation from human pluripotent stem cells via temporal modulation of canonical Wnt signaling. Proc. Natl. Acad. Sci. USA 109, E1848–E1857.

MacDonald, B.T., Tamai, K., and He, X. (2009). Wnt/beta-catenin signaling: components, mechanisms, and diseases. Dev. Cell 17, 9–26.

Middelbeek, J., Clark, K., Venselaar, H., Huynen, M.A., and van Leeuwen, F.N. (2010). The alpha-kinase family: an exceptional branch on the protein kinase tree. Cell. Mol. Life Sci. 67, 875–890.

Moon, J., Zhou, H., Zhang, L.S., Tan, W., Liu, Y., Zhang, S., Morlock, L.K., Bao, X., Palecek, S.P., Feng, J.Q., et al. (2017). Blockade to pathological remodeling of infarcted heart tissue using a porcupine antagonist. Proc. Natl. Acad. Sci. USA 114, 1649–1654.

Moon, R.T., Kohn, A.D., De Ferrari, G.V., and Kaykas, A. (2004). WNT and beta-catenin signalling: diseases and therapies. Nat. Rev. Genet. 5, 691–701.

Naito, A.T., Shiojima, I., Akazawa, H., Hidaka, K., Morisaki, T., Kikuchi, A., and Komuro, I. (2006). Developmental stage-specific biphasic roles of Wnt/beta-catenin signaling in cardiomyogenesis and hematopoiesis. Proc. Natl. Acad. Sci. USA 103, 19812–19817.

Olson, E.N. (2006). Gene regulatory networks in the evolution and development of the heart. Science 313, 1922–1927.

Ozhan, G., and Weidinger, G. (2015). Wnt/β-catenin signaling in heart regeneration. Cell Regen. (Lond.) 4, 3.

Paige, S.L., Thomas, S., Stoick-Cooper, C.L., Wang, H., Maves, L., Sandstrom, R., Pabon, L., Reinecke, H., Pratt, G., Keller, G., et al. (2012). A temporal chromatin signature in human embryonic stem cells identifies regulators of cardiac development. Cell 151, 221–232.

Palpant, N.J., Hofsteen, P., Pabon, L., Reinecke, H., and Murry, C.E. (2015a). Cardiac development in zebrafish and human embryonic stem cells is inhibited by exposure to tobacco cigarettes and e-cigarettes. PLoS One 10, e0126259.

Palpant, N.J., Pabon, L., Roberts, M., Hadland, B., Jones, D., Jones, C., Moon, R.T., Ruzzo, W.L., Bernstein, I., Zheng, Y., et al. (2015b). Inhibition of β-catenin signaling respecifies anterior-like endothelium into beating human cardiomyocytes. Development 142, 3198–3209.

Palpant, N.J., Wang, Y., Hadland, B., Zaunbrecher, R.J., Redd, M., Jones, D., Pabon, L., Jain, R., Epstein, J., Ruzzo, W.L., et al. (2017). Chromatin and transcriptional analysis of mesoderm progenitor cells identifies HOPX as a regulator of primitive hematopoiesis. Cell Rep. 20, 1597–1608.

Peralta, M., Steed, E., Harlepp, S., González-Rosa, J.M., Monduc, F., Ariza-Cosano, A., Cortés, A., Rayón, T., Gómez-Skarmeta, J.L., Zapata, A., et al. (2013). Heartbeat-driven pericardiac fluid forces contribute to epicardium morphogenesis. Curr. Biol. 23, 1726–1735.

Plavicki, J.S., Hofsteen, P., Yue, M.S., Lanham, K.A., Peterson, R.E., and Heideman, W. (2014). Multiple modes of proepicardial cell migration require heartbeat. BMC Dev. Biol. 14, 18.

Ren, J., Wang, R., Huang, G., Song, H., Chen, Y., and Chen, L. (2013). sFRP1 inhibits epithelial-mesenchymal transition in A549 human lung adenocarcinoma cell line. Cancer Biother. Radiopharm. 28, 565–571.

Rossi, A., Kontarakis, Z., Gerri, C., Nolte, H., Hölper, S., Krüger, M., and Stainier, D.Y. (2015). Genetic compensation induced by deleterious mutations but not gene knockdowns. Nature 524, 230–233.

Schulte-Merker, S., and Stainier, D.Y. (2014). Out with the old, in with the new: reassessing morpholino knockdowns in light of genome editing technology. Development 141, 3103–3104.

Serluca, F.C. (2008). Development of the proepicardial organ in the zebrafish. Dev. Biol. 315, 18–27.

Sisson, B.E., Dale, R.M., Mui, S.R., Topczewska, J.M., and Topczewski, J. (2015). A role of glypican4 and wnt5b in chondrocyte stacking underlying craniofacial cartilage morphogenesis. Mech. Dev. 138 (Pt 3), 279–290.

Stainier, D.Y., and Fishman, M.C. (1994). The zebrafish as a model system to study cardiovascular development. Trends Cardiovasc. Med. 4, 207–212.

Stamos, J.L., and Weis, W.I. (2013). The β-catenin destruction complex. Cold Spring Harb. Perspect. Biol. 5, a007898.

Ueno, S., Weidinger, G., Osugi, T., Kohn, A.D., Golob, J.L., Pabon, L., Reinecke, H., Moon, R.T., and Murry, C.E. (2007). Biphasic role for Wnt/beta-catenin signaling in cardiac specification in zebrafish and embryonic stem cells. Proc. Natl. Acad. Sci. USA 104, 9685–9690.

Weidinger, G., Thorpe, C.J., Wuennenberg-Stapleton, K., Ngai, J., and Moon, R.T. (2005). The Sp1-related transcription factors sp5 and sp5-like act downstream of Wnt/beta-catenin signaling in mesoderm and neuroectoderm patterning. Curr. Biol. 15, 489–500.

Woll, P.S., Morris, J.K., Painschab, M.S., Marcus, R.K., Kohn, A.D., Biechele, T.L., Moon, R.T., and Kaufman, D.S. (2008). Wnt signaling promotes hematoendothelial cell development from human embryonic stem cells. Blood 111, 122–131.

Yoshida, Y., Tsunoda, T., Doi, K., Fujimoto, T., Tanaka, Y., Ota, T., Ogawa, M., Matsuzaki, H., Kuroki, M., Iwasaki, A., et al. (2012). ALPK2 is crucial for luminal apoptosis and DNA repair-related gene expression in a three-dimensional colonic-crypt model. Anticancer Res. 32, 2301–2308.

Zeng, X., Tamai, K., Doble, B., Li, S., Huang, H., Habas, R., Okamura, H., Woodgett, J., and He, X. (2005). A dual-kinase mechanism for Wnt co-receptor phosphorylation and activation. Nature 438, 873–877.

Supplemental Information

ALPK2 Promotes Cardiogenesis in Zebrafish

and Human Pluripotent Stem Cells

Peter Hofsteen, Aaron Mark Robitaille, Nicholas Strash, Nathan Palpant, Randall T. Moon, Lil Pabon, and Charles E. Murry

Transparent Methods

Cell culture and cardiac directed differentiation.

Human embryonic stem cells (RUES2) were maintained and cardiac directed differentiation was performed based on methods previously described (Palpant et al., 2015a). Briefly, hESCs were seeded on Matrigel (BD) coated plates and directed differentiation was performed using a combination of activin A and BMP4 and small molecule activation and inhibition of the WNT/β-catenin signaling pathway as illustrated in Figure 1D. Endothelial differentiation was performed as previously described (Palpant et al., 2015b). Briefly, differentiation was initiated with Activin A (100 ng/mL for endocardial-like endothelium (EECs) and 50 ng/mL for hemogenic endothelium (HECs)) in RPMI B27 without insulin and 1x matrigel. On day 1, media was changed to BMP4 (5 ng/mL for EECs and 40 ng/mL for HECs) in RPMI B27 minus insulin with 1 µM CHIR-99021. On day 2 media was changed to Stempro34 (Invitrogen, 10640019) backbone media containing 200 ng/mL VEGF (Peprotech, 100-20), 5 ng/mL bFGF (Peprotech, 100-18B), 10 ng/mL BMP4 (R&D SYSTEMS, 314-BP-050), 4×10^{-4} M monothioglycerol, 50 µg/mL Ascorbic Acid, 2mM L-Glutamine (Invitrogen, 25030-081), and pen-strep (Invitrogen, 15140-163) and remained until day 5 when cells were phenotyped.

Zebrafish strains and husbandry.

Wild-type (AB; zebrafish International Resource Center, Eugene, OR, USA), *tcf21:DsRed2* (Kikuchi et al., 2011), *cmlc2:DsRed-nuc* (Mably et al., 2003), *myl7:GFP* (Burns et al., 2005) and *hsWNT8:GFP* (Weidinger et al., 2005) were used and maintained using standard procedures (Westerfield, 2000) in accordance with the Institutional Animal Care and Use Committee-approved protocols.

Flow Cytometry.

Cardiomyocyte purity and immaturity was assessed by flow cytometry using cardiac troponin T (Thermo Scientific, 1:100) antibody and smooth muscle actin (SMA; Abcam, 1:200) or the isotype control on day 14 of hESC directed differentiation. Human ESC derived endothelial cells were analyzed on day 5 with antibodies against human VEGF

R2/KDR PE (R&D Systems) and CD34 (BD Biosciences, 340430). Cells were analyzed using a BD FACSCANTO II or sorted on a BD FACSARIA II (Beckton Dickinson, San Jose, CA) with FACS Diva software (BD Biosciences). Instrument settings were adjusted to avoid spectral overlap.

Quantitative Reverse Transcriptase PCR (RT-qPCR).

Total RNA isolation was performed as per manufacturers' protocol (RNeasy Miniprep Kit, QIAGEN). First-strand cDNA from 500 ng total RNA was synthesized using the Superscript III enzyme kit (Invitrogen). Quantitative RT-PCR was conducted using the Sensimix SYBR PCR Kit (Bioline) on a 7900HT Fast-Real-Time PCR system (Applied Biosystems). Relative transcript values were normalized to either HPRT (human) or β-actin (zebrafish) and primers are listed in Table S1.

Analysis of RNA-seq and chromatin dynamics.

Figure 1C is based on the following data set: NCBI Gene Expression Omnibus (GEO; GSE35583, epigenetics; GSE19090, gene expression; previously deposited (Paige et al., 2012). Figure 1F is based on the following data set: GEO: GSE97080 (Palpant et al., 2017).

In situ hybridization.

Wild type zebrafish embryos were collected at 13 and 22 hpf, fixed in 4% paraformaldehyde, dehydrated to methanol, and stored at -20°C until needed. A 613 base pair fragment spanning of *alpk2* was amplified from embryonic zebrafish cDNA using primers listed in Table S1 and the digoxigenin-UTP (Roche) antisense *alpk2* riboprobe was synthesized using T7 RNA polymerase (Promega). The *gata4* riboprobe was previously synthesized (Paige et al., 2012) and *in situ* hybridization was performed as previously described (Hofsteen et al., 2013). Images were obtained using a Nikon SMZ1500 microscope using a Nikon Digital DS-Ri1 camera.

Morpholino Oligonucleotides.

Translation and splice blocking morpholino oligonucleotides (MO) (GeneTools LLC,

Philomath, OR) were injected into one-cell zebrafish embryos (0.25-1 ng/embryo). Validation of splicing was confirmed by reverse transcriptase PCR following first strand cDNA synthesis (Invitrogen) using primers designed to amplify the flanking region of intron-exon 4 (f1, r1; exons 4-6) as well as downstream the splice junction (f2, r2; exons 5-6). Primers and MO sequences can be found in Table S1 and validation is illustrated in Figure 2A-D.

CRISPR/Cas9 gene editing

Human and zebrafish guide sequences were designed using CRISPRscan software (Moreno-Mateos et al., 2015) and are listed in Table S1. Human sgRNA oligonucleotides were designed with overhangs for ligation into a BbsI (ThermoFisher Scientific) digested pSpCas9(BB)-2A-Puro (px459) V2.0 (gifted from Feng Zhang, Addgene plasmid # 62988) single vector expression system (Ran et al., 2013). Human PSCs were transfected with 1 µg of the ALPK2 sgRNA-PX459 plasmid using GeneJuice (EMD Millipore and hESCs with plasmid integration were selected using puromycin (InvivoGen). Confirmation of mutation and stop codon was conducted by Sanger sequencing. Zebrafish sgRNA and nCas9 was synthesized, injected, and screed as previously described (Hofsteen et al., 2016). Founder fish (F0) were outcrossed to with wild type AB fish to generate a stable Alpk2 hemizygous line (F1). F1 fish were subsequently propagated and hemizygous fish were bred to attain homozygosity. Validation of mutations were conducted through Sanger sequencing. Guide sequences and primers used for validation are listed in Table S1.

Immunohistochemistry and confocal microscopy.

Zebrafish antibody staining was performed as previously described (Plavicki et al., 2013). Primary antibody used was rabbit anti-DsRed (AnaSpec, Fremont, CA) at 1:200 in phosphate buffered saline with 0.03% triton and 4% bovine serum albumin (PBT) followed by secondary antibody Alexafluor 568 at 1:100 in PBT. Samples were mounted with Vectashield containing DAPI (Vector Laboratories) and images were obtained using a Nikon A1R confocal mounted on a Nikon TiE inverted microscope.

Zebrafish heart rate, cardiomyocyte quantification, and O-dianisidine staining.

Heart rate was collected by counting ventricular contractions from randomly selected fish over a period of one minute at 27˚C (Video S1). Zebrafish (*cmlc2:DsRed-nuc*) were injected with control or *Alpk2* MO, fixed at 48 hpf and processed for IHC as described above. Fish were stained for rabbit anti-DsRed (1:200, AnaSpec, Fremont, CA) and mouse anti-activated leukocyte cell adhesion molecule (ALCAM, 1:50) primary antibodies followed by secondary staining with Alexaflour-596 anti-rabbit and -633 anti-mouse at 1:100. Hearts were imaged (z-series) by confocal microscopy and cardiomyocytes were counted in a blinded fashion. O-dianisidine staining was performed by staining control and Alpk2Δ5 zebrafish at 72 hpf with a o-dianisidine solution (o-dianisidine (0.6 mg/ml), 0.01 M sodium acetate (pH 4.5), 0.65% H202, and 40% (vol/vol) ethanol)) as previously described (Paffett-Lugassy and Zon, 2005). Briefly, fish were dechorionated and stained in the dark for 25 minutes at room temperature, washed 3x with deionized H20 and fixed overnight with 4% paraformaldehyde in PBS (vol/vol) at 4˚C. Embryos were bleached as described (Paffett-Lugassy and Zon, 2005) and imaged using a Nikon SMZ1500 microscope using a Nikon Digital DS-Ri1 camera.

Short hairpin RNA (shRNA) and lentiviral transduction.

Three non-overlapping shRNAs targeting various regions of the ALPK2 transcript were inserted into a PLKO.1 vector containing a puromyocin resistance cassette (TRCN0000230560, NM_05947.3-368s21c1; TRCN0000230561, NM_05947.3-1217s21c1; TCRN0000230562, NM_052947.3-5858s21c1; Sigma, Table S1). Lentivirus was synthesized and cells were transfected in suspension containing 10 µM Y-27632 (Sigma). For control, cells were transduced with a lentivirus containing a non-targeting shRNA (Sigma). Cells were transduced for 48 hours, puromyocin selected and passaged for expansion once prior to cardiac differentiation. To validate the efficiency of ALPK2 knockdown, we transduced cardiomyocytes with three non-overlapping ALPK2 shRNAs. All ALPK2 shRNAs resulted in significant reduction (72-83%) of ALPK2 when compared to the empty vector shRNA controls (Figure 4B). For assessing WNT/β-catenin activity, hESCs were transduced with a lentiviral β-catenin-activated reporter (BAR) driving venus as previously reported (Palpant et al., 2015b).

Western Blotting

Cells were lysed in ice-cold cell lysis buffer (Cell Signaling, cat# 9803) containing protease inhibitors (Calbiochem, cat# 539134) and quantification of total protein was conducted using the Pierce BCA Protein Assay Kit (Thermo Scientific). Normalized total protein was subjected to SDS-PAGE and western blotting was performed as previously described (Yang et al., 2014). Primary antibodies used are listed below were coupled with either anti-mouse, anti-goat or anti rabbit horseradish peroxidase secondary antibody at 1:5000 (Santa Cruz Biotechnology).

	Manufacturer	Host	Dilution	Lot
CTNNB1	Cell Signaling	Rabbit	1 / 1000	9562S
LRP6	Cell Signaling	Rabbit	1 / 1000	3395
phospho-LRP6 (S1490)	Cell Signaling	Rabbit	1 / 1000	2568
LEF1	Cell Signaling	Rabbit	1 / 1000	2230
PKN2	Bethyl Labs	Rabbit	1 / 1000	A302-443A
SCRIB	Santa Cruz	Goat	1 / 1000	sc-11049
GAPDH	Abcam	Mouse	1 / 5000	ab8245

Proteomics

Label Free Quantitative Proteomics was conducted as previously published (Hofsteen et al., 2016) and described in detail in the supplemental experimental procedures. In brief, hESCs, CPCs and cardiomyocytes treated with either control or ALPK2 shRNA (2 biological replicates per time point/treatment) were pooled and washed in 1xPBS and flash frozen. Cell pellets were lysed in 1M urea, 50mM ammonium bicarbonate, pH 7.8, and heated to 50°C for 20min. Cell debris was removed by centrifugation (1000g, 2min). Following a BCA assay, normalized quantities of protein were reduced with 2mM DTT, alkylated with 15mM iodoacetamide, and digested overnight with a 1:50 ratio of trypsin to total protein. The resulting peptides were desalted on Waters Sep-Pak C18 cartridges. Peptides were measured by nano-LC-MS/MS on a Thermo Scientific Fusion Orbitrap. Peptides were separated online by reverse phase chromatography using a heated 50°C 30cm C18 column (75mm ID packed with Magic C18 AQ 3μM /100Å

beads) in a 180min gradient (1% to 45% acetonitrile with 0.1% formic acid) separated at 250nL/min. The Fusion Orbitrap was operated in data-dependent mode with the following settings: 60000 resolution, 400-1600 m/z full scan, Top Speed 3 seconds, and an 1.8 m/z isolation window. Identification and label free quantification (LFQ intensity) of peptides was done with MaxQuant 1.5 using a 1% false discovery rate (FDR) against the human Swiss-Prot/TrEMB database downloaded from Uniprot on October 11th, 2013. The databases contained forward and reverse human sequences as well as common contaminants. Peptides were searched using a 5 ppm mass error and a match between run window of 2 min. Proteins that were significantly regulated between conditions were identified using a permutation-based t-test (S1, FDR 5%) in Perseus

SILAC Proteomics: Undifferentiated RUES2 cells were metabolically labeled in conditioned media containing R0K0 (light) or R10K8 (heavy) SILAC DMEM/F-12 media (Dundee Cells Products) for 6 passages. Cells were then differentiated into cardiomyocytes in R0K0 (light) or R10K8 (heavy) RPMI SILAC media (Dundee Cells Products). Cells were washed in 1xPBS and flash frozen. Cell pellets were lysed in 1M urea, 50mM ammonium bicarbonate, pH 7.8, and heated to 50°C for 20min. Cell debris was removed by centrifugation (1000g, 2min). Following a BCA assay, normalized quantities of protein were reduced with 2mM DTT, alkylated with 15mM iodoacetamide, and digested overnight with a 1:50 ratio of trypsin to total protein. The resulting peptides were desalted on Waters Sep-Pak C18 cartridges. Phosphopeptides were then enriched using Pierce Titanium Dioxide Phosphopeptide Enrichment Kit (Thermo Fisher Scientific) according to the manufactures instructions. Peptides were measured by nano-LC-MS/MS on a Fusion Orbitrap (Thermo Fisher Scientific). Peptides were separated online by reverse phase chromatography using a heated 50°C 30cm C18 columns (75mm ID packed with Magic C18 AQ 3μM /100Å beads) in a 180min gradient (1% to 45% acetonitrile with 0.1% formic acid) separated at 250nL/min. The Fusion was operated in data-dependent mode with the following settings: 60000 resolution, 400-1600 m/z full scan, Top Speed 3 seconds, and an 1.8 m/z isolation window. Identification and label free quantification of peptides was done with MaxQuant 1.5 using a 1% false discovery rate (FDR) against the human Swiss-Prot/TrEMB database

downloaded from Uniprot on June 2nd, 2016. The databases contained forward and reverse human sequences as well as common contaminants. We analyzed two biological replicates per condition with six technical replicates. Peptides were searched using a 5ppm mass error and a match between run window of 2min. Gene ontology term analysis was conducted using DAVID functional analysis.

Statistics. Single variable analysis between two samples was carried out using Student's t-test. Single and multivariable assays were analyzed by one- or two-way ANOVA. Results are presented as mean±SEM. For all statistically significant results, *P<0.05.
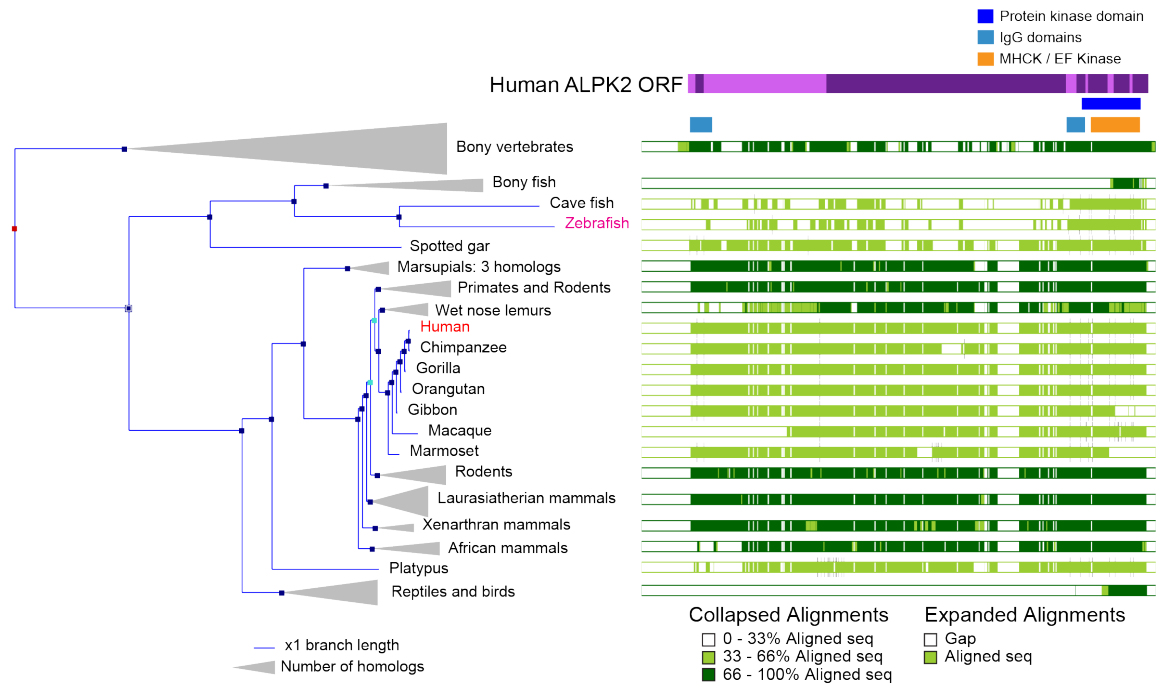
Figure S1: ALPK2 conservation and sequence alignment modified from ensembl. Related to figure 1.
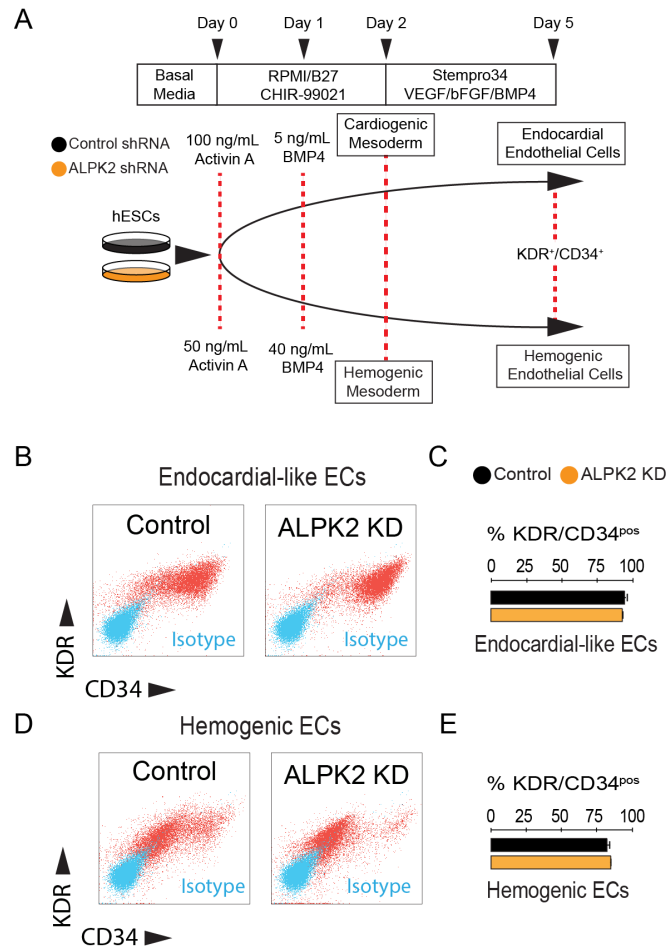
Figure S2: ALPK2 is dispensable for human endocardial and hemogenic endothelial cell differentiation. (A) Schematic of the directed differentiation protocols from human embryonic stem cells towards endocardial-like endothelial cells and hemogenic endothelial cells following control or ALPK2 shRNA transfection. (B, D) Representative flow cytometry scatter plots (B, D; y-axis; VEGF receptor 2 (KDR/FLK1), x-axis; CD34) and quantification (C, E) of control and ALPK2 shRNA knockdown endocardial-like and hemogenic endothelial progenitor cell populations at day 5 of the protocol illustrated in panel A. N=3 biological replicates, Data are mean ±SEM, data were not determined significantly significant by Students t-test. Related to figure 4
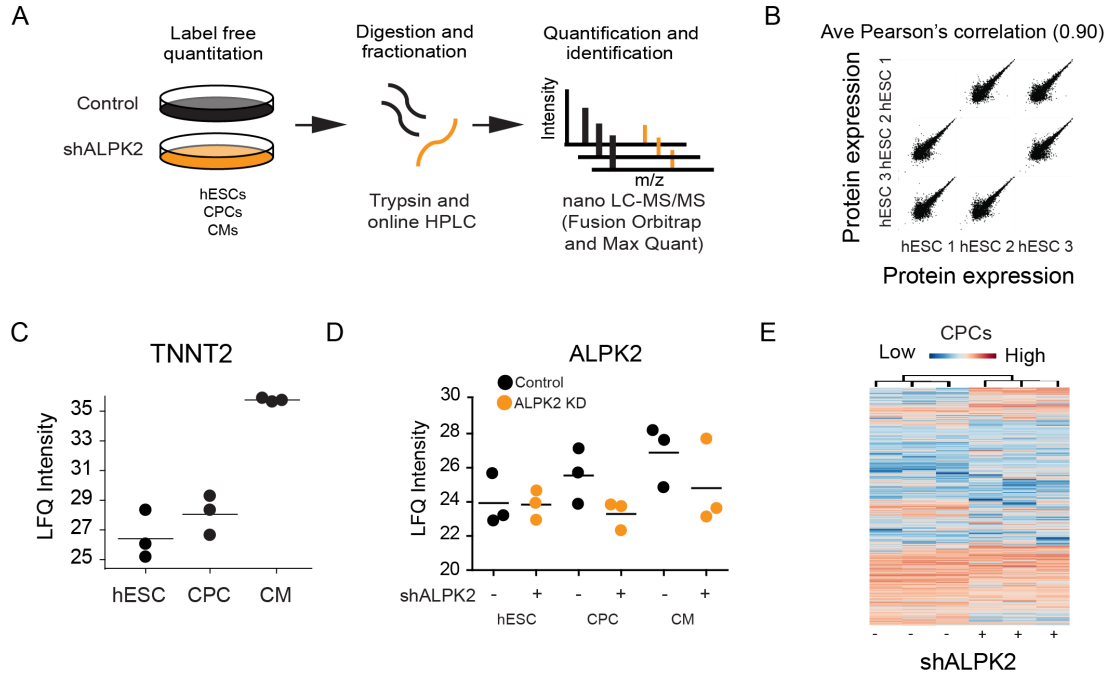
Figure S3: Label free quantitative (LFQ) proteomics of control and ALPK2 shRNA human embryonic stem cells (hESC) differentiated towards cardiac progenitor cells (CPC) and cardiomyocytes (CM). (A) Schematic of LFQ proteomic workflow and reproducibility (B). (C) Protein expression (LFQ intensity) of TNNT2 in hESCs, CPCs and cardiomyocytes (CM). (D) ALPK2 expression over time course cardiomyocyte differentiation and following ALPK2 knockdown. (E) Hierarchical clustering of total protein expression by heat map analysis. Data is representative of 2 biological replicates that were pooled, processed and measured in triplicate. Data were not determined significantly significant by Students t-test. Related to figure 4.
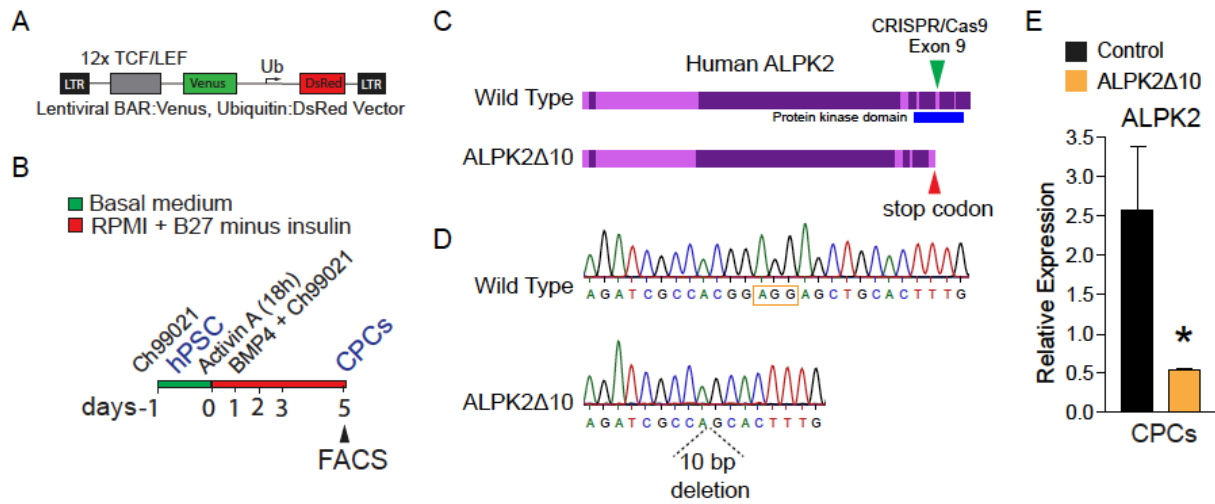
Figure S4: β-catenin-activated-reporter (BAR) assay and CRISPR/Cas9 mutagenesis in human embryonic stem cells (hESC). (A) Depiction of BAR construct to express venus during active β-catenin binding to TCF/LEF elements. (B) Differentiation protocol used to survey BAR activity. (C) Schematic of human ALPK2 locus and CRISPR/Cas9 mutagenesis and (D) Sanger sequencing of wild type (upper) and mutant ALPK2 (ALPK2Δ10, lower) and RT-qPCR (E) for *ALPK2* in wild type and ALPK2Δ10 cardiac progenitor cells derived from human pluripotent stem cells. N=3 biological replicates and data are displayed as mean±SEM. * = p≤0.05. Related to figure 5.

A

B

0.672

0.672

Ave Ratio H/L Ave Ratio H/L normalized #1

10

0

10

0

Ave Ratio H/L normalized #1   Ave Ratio H/L normalized #2

Pearson's Correlation

1.0
0.9
0.8
0.7
0.6

Technical Reproducibility

C

GO Terms Repressed

Extracellular matrix organization
Platelet-derived growth factor binding
Extracellular matrix structural constituent
Collagen catabolic process
Cellular response to amino acid stimulus
Response to L-ascorbic acid
Actin filament binding
Protein binding
Response to cadmium ion
Endodermal cell differentiation
Basement membrane organization
Platelet activation
Collagen fibril organization
Wound healing
Metal ion binding
Poly(A) RNA binding
Protein heterotrimerization
Cell-matrix adhesion
Response to hyperoxia
Negative regulation of Wnt signaling pathwayv
Platelet degranulation
Cytoskeleton organization
Regulation of transcription, DNA-templated
Regulation of catalytic activity
Heart development
Negative regulation of DNA binding
Nucleotide binding
Protein binding, bridging
β-catenin binding
Regulation of synaptic plasticity
Blood coagulation, fibrin clot formation
Blood vessel development
Ureteric bud development
Muscle filament sliding
Cell adhesion
Transcriptional activator activity
Structural constituent of muscle
SMAD binding
Histone H3-K27 trimethylation
Collagen-activated tyrosine kinase receptor signaling
Collagen biosynthetic process
Response to activity
Protein kinase C binding

GO Terms Enriched

Protein binding
Cadherin binding involved in cell-cell adhesion
Cell-cell adhesion
Poly(A) RNA binding
Actin crosslink formation
Negative regulation of androgen receptor signaling pathway
β-catenin-TCF complex assembly
Sister chromatid cohesion
Glycogen catabolic process
Viral process
GTPase binding
positive regulation of filopodium assembly
RNA polymerase II repressing transcription factor binding
Response to axon injury
Fungiform papilla formation
Actin filament bundle assembly
Cell division
Protein complex binding
Retrograde vesicle-mediated transport, Golgi to ER
Epoxide hydrolase activity
Positive regulation of interleukin-1 production
Positive regulation of PERK-mediated unfolded protein response
Microtubule-based process
Negative regulation of B cell differentiation
Negative regulation of peptidyl-lysine acetylation
Establishment of protein localization to plasma membrane
Hair follicle placode formation
Negative regulation of canonical Wnt signaling pathway

0.00   p-value   0.05

Figure S5: SILAC proteomics reproducibility and GO term analysis. (A, B) Pearson's correlation between biological replicates. (C) Gene ontology (GO) enrichment analysis of upregulated and downregulated proteins as a result of ALPK2 mutagenesis in cardiac progenitor cells derived from human embryonic stem cells. Related to figure 6.

SUPPLEMENTAL TABLES

Table S1: Human and zebrafish oligonucleotides using for gene targeting and RT-qPCR. Related to Figures 1, 2, 3, 4, and 5.

Table S2: All proteins identified by label-free quantitative (LFQ) proteomics. Related to Figure 4

Table S3: ALPK2 regulated proteins identified by label-free quantitative (LFQ) proteomics in cardiac progenitor cells. Related to Figure 4

Table S4: GO Terms enriched by ALPK2 knockdown identified by label-free quantitative (LFQ) proteomics in cardiac progenitor cells. Related to Figure 4.

Table S5: GO Terms repressed by ALPK2 knockdown identified by label-free quantitative (LFQ) proteomics in cardiac progenitor cells. Related to Figure 4.

Table S6: All proteins identified by stable isotope labelling of amino acids in cell culture (SILAC) proteomics. Related to Figure 6.

Table S7: GO Terms enriched in ALPK2Δ10 cardiac progenitor cells identified by stable isotope labelling of amino acids in cell culture (SILAC) proteomics. Related to Figure 6.

Table S8: GO Terms repressed in ALPK2Δ10 cardiac progenitor cells identified by stable isotope labelling of amino acids in cell culture (SILAC) proteomics. Related to Figure 6.

Table S9: All phosphopeptides identified and differentially phosphorylated in ALPK2Δ10 cardiac progenitor cells identified by stable isotope labelling of amino acids in cell culture (SILAC) proteomics. Related to Figure 6.

REFERENCES

Burns, C.G., Milan, D.J., Grande, E.J., Rottbauer, W., MacRae, C.A., and Fishman, M.C. (2005). High-throughput assay for small molecules that modulate zebrafish embryonic heart rate. Nat Chem Biol *1*, 263-264.

Hofsteen, P., Plavicki, J., Johnson, S.D., Peterson, R.E., and Heideman, W. (2013). Sox9b is required for epicardium formation and plays a role in TCDD-induced heart malformation in zebrafish. Mol Pharmacol *84*, 353-360.

Hofsteen, P., Robitaille, A.M., Chapman, D.P., Moon, R.T., and Murry, C.E. (2016). Quantitative proteomics identify DAB2 as a cardiac developmental regulator that inhibits WNT/β-catenin signaling. Proc Natl Acad Sci U S A.

Kikuchi, K., Gupta, V., Wang, J., Holdway, J.E., Wills, A.A., Fang, Y., and Poss, K.D. (2011). tcf21+ epicardial cells adopt non-myocardial fates during zebrafish heart development and regeneration. Development *138*, 2895-2902.

Mably, J.D., Mohideen, M.A., Burns, C.G., Chen, J.N., and Fishman, M.C. (2003). heart of glass regulates the concentric growth of the heart in zebrafish. Curr Biol *13*, 2138-2147.

Moreno-Mateos, M.A., Vejnar, C.E., Beaudoin, J.D., Fernandez, J.P., Mis, E.K., Khokha, M.K., and Giraldez, A.J. (2015). CRISPRscan: designing highly efficient sgRNAs for CRISPR-Cas9 targeting in vivo. Nat Methods *12*, 982-988.

Paffett-Lugassy, N.N., and Zon, L.I. (2005). Analysis of hematopoietic development in the zebrafish. Methods Mol Med *105*, 171-198.

Paige, S.L., Thomas, S., Stoick-Cooper, C.L., Wang, H., Maves, L., Sandstrom, R., Pabon, L., Reinecke, H., Pratt, G., Keller, G.*, et al.* (2012). A temporal chromatin signature in human embryonic stem cells identifies regulators of cardiac development. Cell *151*, 221-232.

Palpant, N.J., Hofsteen, P., Pabon, L., Reinecke, H., and Murry, C.E. (2015a). Cardiac development in zebrafish and human embryonic stem cells is inhibited by exposure to tobacco cigarettes and e-cigarettes. PLoS One *10*, e0126259.

Palpant, N.J., Pabon, L., Roberts, M., Hadland, B., Jones, D., Jones, C., Moon, R.T., Ruzzo, W.L., Bernstein, I., Zheng, Y.*, et al.* (2015b). Inhibition of β-catenin signaling respecifies anterior-like endothelium into beating human cardiomyocytes. Development.

Palpant, N.J., Wang, Y., Hadland, B., Zaunbrecher, R.J., Redd, M., Jones, D., Pabon, L., Jain, R., Epstein, J., Ruzzo, W.L.*, et al.* (2017). Chromatin and Transcriptional Analysis of Mesoderm Progenitor Cells Identifies HOPX as a Regulator of Primitive Hematopoiesis. Cell Rep *20*, 1597-1608.

Plavicki, J., Hofsteen, P., Peterson, R.E., and Heideman, W. (2013). Dioxin inhibits zebrafish epicardium and proepicardium development. Toxicol Sci *131*, 558-567.

Ran, F.A., Hsu, P.D., Wright, J., Agarwala, V., Scott, D.A., and Zhang, F. (2013). Genome engineering using the CRISPR-Cas9 system. Nat Protoc *8*, 2281-2308.

Weidinger, G., Thorpe, C.J., Wuennenberg-Stapleton, K., Ngai, J., and Moon, R.T. (2005). The Sp1-related transcription factors sp5 and sp5-like act downstream of Wnt/beta-catenin signaling in mesoderm and neuroectoderm patterning. Curr Biol *15*, 489-500.

Westerfield, M. (2000). The Zebrafish book. A guide for the laboratory use of zebrafish (*Danio rerio*), 4th ed edn (Eugene, OR: Univ. of Oregon Press).

Yang, X., Rodriguez, M., Pabon, L., Fischer, K.A., Reinecke, H., Regnier, M., Sniadecki, N.J., Ruohola-Baker, H., and Murry, C.E. (2014). Tri-iodo-l-thyronine promotes the maturation of human cardiomyocytes-derived from induced pluripotent stem cells. J Mol Cell Cardiol *72*, 296-304.